EUROPEAN ORGANISATION FOR NUCLEAR RESEARCH (CERN)

Search for non-pointing and delayed photons in the diphoton and missing transverse momentum final state in 8 TeV pp collisions at the LHC using the ATLAS detector

The ATLAS Collaboration

Abstract

A search has been performed, using the full data sample of 20.3 fb^{-1} of 8 TeV proton–proton collisions collected in 2012 with the ATLAS detector at the LHC, for photons originating from a displaced vertex due to the decay of a neutral long-lived particle into a photon and an invisible particle. The analysis investigates the diphoton plus missing transverse momentum final state, and is therefore most sensitive to pair-production of long-lived particles. The analysis technique exploits the capabilities of the ATLAS electromagnetic calorimeter to make precise measurements of the flight direction, as well as the time of flight, of photons. No excess is observed over the Standard Model predictions for background. Exclusion limits are set within the context of Gauge Mediated Supersymmetry Breaking models, with the lightest neutralino being the next-to-lightest supersymmetric particle and decaying into a photon and gravitino with a lifetime in the range from 250 ps up to about 100 ns.

Search for non-pointing and delayed photons in the diphoton and missing transverse momentum final state in 8 TeV pp collisions at the LHC using the ATLAS detector

The ATLAS Collaboration

A search has been performed, using the full 20.3 fb^{-1} data sample of 8 TeV proton–proton collisions collected in 2012 with the ATLAS detector at the LHC, for photons originating from a displaced vertex due to the decay of a neutral long-lived particle into a photon and an invisible particle. The analysis investigates the diphoton plus missing transverse momentum final state, and is therefore most sensitive to pair-production of long-lived particles. The analysis technique exploits the capabilities of the ATLAS electromagnetic calorimeter to make precise measurements of the flight direction, as well as the time of flight, of photons. No excess is observed over the Standard Model predictions for background. Exclusion limits are set within the context of Gauge Mediated Supersymmetry Breaking models, with the lightest neutralino being the next-to-lightest supersymmetric particle and decaying into a photon and gravitino with a lifetime in the range from 250 ps to about 100 ns.

I. INTRODUCTION

This article reports the results of a search for photons originating from a displaced vertex due to the decay of a neutral long-lived particle into a photon and an invisible particle. The search exploits the capabilities of the ATLAS liquid-argon (LAr) electromagnetic (EM) calorimeter to make precise measurements of the flight direction and the time of flight of photons. The analysis uses the full data sample of 8 TeV proton–proton (pp) collisions collected in 2012 with the ATLAS detector at the CERN Large Hadron Collider (LHC), corresponding to an integrated luminosity of 20.3 fb^{-1}. The method used is an evolution of the ATLAS non-pointing photon analysis [1] using the full 2011 data sample of 7 TeV pp collisions, corresponding to an integrated luminosity of 4.8 fb^{-1}. This previous analysis based on 7 TeV pp collisions found no excess above the Standard Model (SM) background expectation.

Scenarios where neutral long-lived particles are produced in pairs arise naturally, for example, within models of supersymmetry (SUSY) [2–10]. SUSY predicts the existence of a new SUSY partner (sparticle) for each of the SM particles, with identical quantum numbers except differing by half a unit of spin. In R-parity-conserving SUSY models [11–15], pp collisions at the LHC could produce these sparticles in pairs, and they would then decay in cascades involving other sparticles and SM particles until the lightest SUSY particle (LSP) is produced, which is stable. This analysis investigates the diphoton plus large $E_{\mathrm{T}}^{\mathrm{miss}}$ final state, where $E_{\mathrm{T}}^{\mathrm{miss}}$ is the magnitude of the missing transverse momentum, and is therefore most sensitive to the pair-production of long-lived particles.

In gauge-mediated supersymmetry breaking (GMSB) models [16–21], the gravitino ($\tilde{G}$) is the LSP and is predicted, for typical model parameter values, to be very light. While the recent discovery of a Higgs boson with a mass around 125 GeV [22, 23] disfavors minimal GMSB within reach of the LHC, modifications to minimal GMSB can easily accommodate this Higgs mass value without changing the sparticle masses [24–26]. GMSB phenomenology is largely determined by the properties of the next-to-lightest supersymmetric particle (NLSP), since the decay chains of the sparticles with higher mass would terminate in the decay of the NLSP. Very weak coupling of the NLSP to the gravitino could lead to displaced decay vertices of the NLSP [20]. The NLSP lifetime (τ) depends on the fundamental scale of SUSY breaking [27, 28], and therefore provides important information about the SUSY-breaking mechanism.

The results of this analysis are presented within the context of the so-called Snowmass Points and Slopes parameter set 8 (SPS8) [29], which describes a set of minimal GMSB models with the lightest neutralino ($\tilde{\chi}_1^0$) as the NLSP. The free parameter in the GMSB SPS8 set of models is the effective scale of SUSY breaking, denoted Λ, which depends on details of how the SUSY breaking is communicated to the messenger sector of the theory.

For Λ values below about 100 TeV, strong production of pairs of squarks and/or gluinos make a significant contribution to the production rate of SUSY events at the LHC. However, for most of the range of Λ values relevant for this analysis, SUSY production is dominated by electroweak pair production of gauginos, and in particular of $\tilde{\chi}_2^0\tilde{\chi}_1^\pm$ and $\tilde{\chi}_1^+\tilde{\chi}_1^-$ pairs.

In the GMSB SPS8 models, the dominant decay mode of the NLSP is $\tilde{\chi}_1^0 \to \gamma + \tilde{G}$, leading to a $\gamma\gamma + E_{\mathrm{T}}^{\mathrm{miss}} + X$ final state, where the escaping gravitinos give rise to $E_{\mathrm{T}}^{\mathrm{miss}}$, and X represents SM particles produced in the decay cascades. To minimize the dependence of the results on the details of the SUSY decays, the analysis requires only a pair of photons and large $E_{\mathrm{T}}^{\mathrm{miss}}$, avoiding explicit requirements on the presence of leptons or jets or any other particular SM particles in the final state.

This analysis considers the scenario where the NLSP has a finite lifetime, at least 250 ps, and travels partway through the ATLAS detector before decaying. In

the range of Λ values of interest, about 80–300 TeV, the NLSP mass lies in the range of about 120–440 GeV. In this case, the photons produced in the NLSP decays can either be "non-pointing" or "delayed" or both; namely, the photons can have flight paths that do not point back to the primary vertex (PV) of the event and arrival times at the calorimeter that are later than those expected for a photon produced promptly at the PV.

The search for non-pointing and delayed photons is performed using the excellent performance of the finely segmented LAr EM calorimeters. An EM shower produced by a photon is measured precisely with varying lateral segmentation in three different longitudinal (i.e. depth) segments, allowing a determination of the flight direction of the photon from the EM shower measurements. The flight direction can then be compared with the direction back toward the PV identified for the event. This method is employed to determine the value of the pointing-related variable used, namely $|\Delta z_\gamma|$, defined as the separation, measured along the beamline, between the extrapolated origin of the photon and the position of the selected PV of the event. The LAr calorimeter also has excellent time resolution and the arrival time t_γ of a photon at the calorimeter (with zero defined as the expected value for a prompt photon from the hard collision) is also a sensitive measure, since positive and finite time values would be expected for photons arising from non-prompt NLSP decays.

In the 7 TeV analysis [1], the pointing measurement was used to extract the result, with the time measurement used only qualitatively as a cross-check. The 7 TeV analysis set exclusion limits within the context of GMSB SPS8 models and similar results were obtained in a CMS analysis [30] of their full 7 TeV dataset, but investigating a final state with at least one photon, at least three jets, and $E_{\mathrm{T}}^{\mathrm{miss}}$. The current analysis utilizes both the pointing and time measurements. As described in Sec. VII, the current analysis divides the sample into six exclusive categories, according to the value of $|\Delta z_\gamma|$, and then simultaneously fits the t_γ distributions of each of the categories to determine the possible contribution from signal. The use of both variables greatly improves the sensitivity.

II. THE ATLAS DETECTOR

The ATLAS detector [31] covers nearly the entire solid angle[1] around the collision point and consists of an inner tracking detector surrounded by a solenoid, EM and hadronic calorimeters, and a muon spectrometer incorporating three large toroidal magnet systems. The inner-detector system (ID) is immersed in a 2 T axial magnetic field, provided by a thin superconducting solenoid located before the calorimeters, and provides charged-particle tracking in the pseudorapidity range $|\eta| < 2.5$. The ID consists of three detector subsystems, beginning closest to the beamline with a high-granularity silicon pixel detector, followed at larger radii by a silicon microstrip tracker and then a straw-tube-based transition radiation tracker. The ID allows an accurate reconstruction of tracks from the primary pp collision and precise determination of the location of the PV.

This analysis relies heavily on the capabilities of the ATLAS calorimeter system, which covers the pseudorapidity range $|\eta| < 4.9$. Finely segmented lead/LAr EM sampling calorimeters cover the barrel ($|\eta| < 1.475$) and endcap ($1.375 < |\eta| < 3.2$) regions. An additional thin LAr presampler covering $|\eta| < 1.8$ allows corrections for energy losses in material upstream of the EM calorimeters. Hadronic calorimetry is provided by a steel/scintillator-tile calorimeter, segmented into three barrel structures within $|\eta| < 1.7$, and two copper/LAr hadronic endcap calorimeters. The solid angle coverage is completed with forward copper/LAr and tungsten/LAr calorimeter modules, optimized for EM and hadronic measurements, respectively. Outside the calorimeters lies the muon spectrometer, which identifies muons and measures their deflection up to $|\eta| = 2.7$ in a magnetic field generated by superconducting air-core toroidal magnet systems.

A. Pointing resolution

For $|\eta| < 2.5$, the EM calorimeter is segmented into three layers in depth that are used to measure the longitudinal profile of the shower. The first layer uses highly granular "strips" segmented in the η direction, designed to allow efficient discrimination between single photon showers and two overlapping showers, the latter originating, for example, from the decay of a π^0 meson. The second layer collects most of the energy deposited in the calorimeter by EM showers initiated by electrons or photons. Very high energy showers can leave significant energy deposits in the third layer, which can also be used to correct for energy leakage beyond the EM calorimeter.

By measuring precisely the centroids of the EM shower in the first and second EM calorimeter layers, the flight direction of photons can be determined, from which one can calculate the value of z_{origin}, defined as the z-coordinate of the photon projected back to the point giving its distance of closest approach to the beamline ($x = y = 0$). The angular resolution of the EM calorimeter's measurement of the flight direction of prompt photons is about 60 mrad$/\sqrt{(E/\mathrm{GeV})}$, where E is the photon energy. This angular precision corresponds, in the EM barrel calorimeter, to a resolution in z_{origin} of about

---

[1] ATLAS uses a right-handed coordinate system with its origin at the nominal interaction point (IP) in the center of the detector and the z-axis along the beam pipe. The x-axis points from the IP to the center of the LHC ring, and the y-axis points upward. Cylindrical coordinates (r, ϕ) are used in the transverse plane, ϕ being the azimuthal angle around the beam pipe. The pseudorapidity is defined in terms of the polar angle θ as $\eta = -\ln\tan(\theta/2)$, and the transverse energy as $E_{\mathrm{T}} = E\sin\theta$.

15 mm for prompt photons with energies in the range of 50–100 GeV. Given the geometry, the z resolution is worse for photons reconstructed in the endcap calorimeters, so the pointing analysis is restricted to photon candidates in the EM barrel calorimeter.

In the ATLAS $H \to \gamma\gamma$ analysis [22] that contributed to the discovery of a Higgs boson, this capability of the EM calorimeter was used to help choose the PV from which the two photons originated, thereby improving the diphoton invariant mass resolution and the sensitivity of the search. The analysis described in this paper uses the measurement of the photon flight direction to search for photons that do not point back to the PV. The pointing variable used in the analysis is Δz_γ, defined as the difference between $z_{\rm origin}$ and $z_{\rm PV}$, the z-coordinate of the selected PV of the event. Given that $z_{\rm PV}$ is measured with high precision using the tracker, the $z_{\rm origin}$ resolution is essentially equivalent to the resolution in Δz_γ.

While the geometry of the EM calorimeter is optimized for detecting particles that point back to near the nominal interaction point at the center of the detector (i.e. $x = y = z = 0$), the fine segmentation allows good pointing performance to be achieved over a wide range of photon impact angles. Figure 1 shows the expected pointing resolution (ie. the resolution of the measured $z_{\rm origin}$) as a function of $|z_{\rm origin}|$, for GMSB SPS8 signal photons in the EM barrel calorimeter. The results are obtained from Monte Carlo (MC) simulations (see Sec. III) by fitting to a Gaussian function the difference between the values of $z_{\rm origin}$ obtained from the calorimeter measurement and the MC generator-level information. The pointing resolution degrades with increasing $|z_{\rm origin}|$, but remains much smaller than $|z_{\rm origin}|$ in the region where the signal is expected.

The calorimeter pointing performance was verified in data by using the finite spread of the LHC collision region along the z-axis. The pointing resolution achieved for a sample of electrons from $Z \to ee$ events is also shown in Fig. 1, where the distance, $z_{\rm PV}$, between the PV and the nominal center of the detector serves the role of $z_{\rm origin}$. In this case, the pointing resolution is obtained by fitting to a Gaussian the difference between $z_{\rm PV}$, obtained from reconstructed tracks, and the calorimeter measurement of the origin along the beamline of the electron. Figure 1 shows that a similar pointing performance is observed for photons and for electrons, as expected given their similar EM shower developments. This similarity validates the use of a sample of electrons from $Z \to ee$ events to study the pointing performance for photons. The expected pointing performance for electrons in a MC sample of $Z \to ee$ events is also shown on Fig. 1, and is consistent with the data. The level of agreement between MC simulation and data over the range of values that can be accessed in the data gives confidence in the extrapolation using MC simulation to the larger $|z_{\rm origin}|$ values characteristic of signal photons.
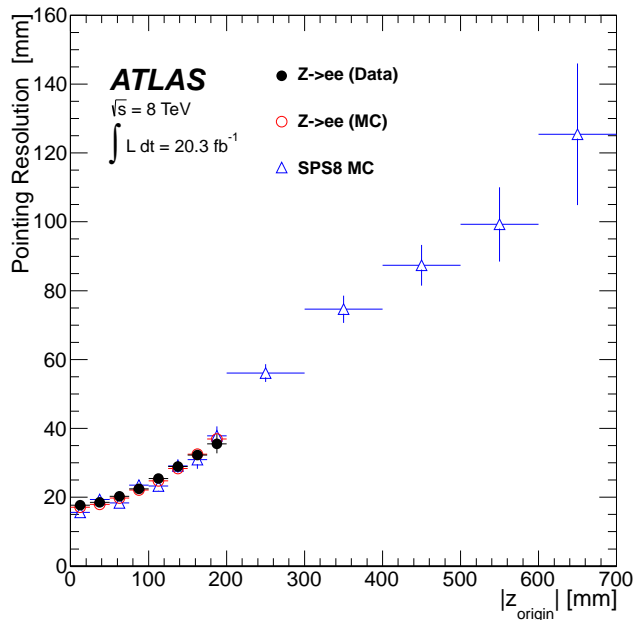

FIG. 1. The pointing resolution (defined as the resolution of $z_{\rm origin}$) obtained for EM showers in the LAr EM barrel calorimeter. The pointing resolution for photons from GMSB SPS8 signal MC samples is plotted as a function of $|z_{\rm origin}|$. The pointing resolution is also shown for $Z \to ee$ data and MC events, for which the PV position, $z_{\rm PV}$, serves the role of $|z_{\rm origin}|$.

B. Time resolution

Photons from long-lived NLSP decays would reach the LAr calorimeter with a slight delay compared to prompt photons produced directly in the hard scatter. This delay results mostly from the flight time of the heavy NLSP, which would have a distribution of relativistic speed ($\beta = v/c$) that peaks typically near 0.9 and has a tail to much lower values. In addition, the opening angle in the NLSP decay, which causes the photon to be non-pointing, results in a longer geometrical path to the calorimeter, as compared to a prompt photon from the PV.

The EM calorimeter, with its novel "accordion" design, and its readout, which incorporates fast shaping, has excellent time resolution. Quality-control tests during production of the electronics required the clock jitter on the LAr readout boards to be less than 20 ps, with typical values of 10 ps [32]. Calibration tests of the overall electronic readout performed *in situ* in the ATLAS cavern show a time resolution of ≈ 70 ps [33], limited not by the readout but by the jitter of the calibration pulse injection system. Test-beam measurements [34] of EM barrel calorimeter modules demonstrated a time resolution of ≈ 100 ps in response to high-energy electrons.

The LAr energy and time for each calorimeter cell are reconstructed by applying the optimal filtering algorithm [35] to the set of five samples of the signal

shape read out for each calorimeter channel, with successive samples on the waveform separated by 25 ns. More specifically, the deposited energy per cell and the time of the deposition are calculated using appropriately weighted linear combinations of the set of samples of the waveform:

$$E = \sum_{i=0}^{4} a_i S_i \quad \text{and} \quad t = \frac{1}{E} \sum_{i=0}^{4} b_i S_i \;, \tag{1}$$

where S_i denotes the five samples of the signal waveform. The parameters a_i and b_i are the optimal filter coefficients (OFC), the values of which are calculated, knowing the pulse shape and noise autocorrelation matrix, to deliver the best energy and time resolutions.

For this analysis, the arrival time of an EM shower is measured using the second-layer EM calorimeter cell with the maximum energy deposit. For the EM shower of an electron or photon with energy within the range of interest, this cell typically contains about $(20–50)\%$ of the total energy deposited in the EM shower. In principle, the times measured in neighboring cells could be used in a weighted time calculation to try to further improve the precision. However, some studies that investigated more complicated algorithms found no improvement in time resolution, likely due to the pulse shapes in the channels with lower deposited energies suffering some distortion due to crosstalk effects.

During 2012, the various LAr channels were timed-in online with a precision of order 1 ns. A large sample of $W \to e\nu$ events in the 8 TeV dataset was used to determine calibration corrections that need to be applied to optimize the time resolution for EM clusters. The calibration includes corrections of various offsets in the time of individual channels, corrections for the energy dependence of the time measurement, crosstalk corrections, and flight-path corrections depending on the PV position.

To cover the full dynamic range of physics signals of interest, the ATLAS LAr calorimeter readout boards [32] employ three overlapping linear gain scales, dubbed High, Medium and Low, where the relative gain is reduced by a factor of about ten for each successive scale. For a given event, any individual LAr readout channel is digitized using the gain scale that provides optimal energy resolution, given the energy deposited in that calorimeter cell. The calibration of the time was determined separately for High and Medium gain for each channel. The number of electron candidates from the $W \to e\nu$ sample that were digitized using Low gain was insufficient to obtain statistically precise results for the calibration constants. Therefore, the analysis requires that selected photons be digitized using either High or Medium gain resulting in a loss in signal efficiency, which ranges from much less than 1%, for the lowest Λ values probed, to less than 5% for the highest Λ values. The majority of signal photons are digitized using Medium gain, the fraction rising with

rising Λ from about 60% to about 90%, over the Λ range of interest.

An independent sample of $Z \to ee$ events was used to validate the time calibration and determine the resolution obtained, by performing Gaussian fits to the time distributions in bins of cell energy. Figure 2 shows the time resolution for High and Medium gain cells with $|\eta| < 0.4$, as a function of the energy in the second-layer calorimeter cell used to calculate the time for the sample of $Z \to ee$ events. Similar results are obtained over the full coverage of the EM calorimeter.
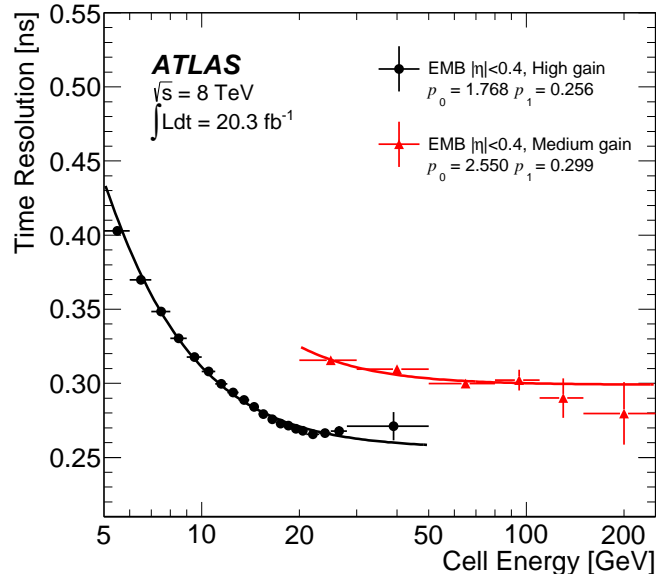

FIG. 2. Time resolution, as a function of the energy in the second-layer cell with the maximum energy, obtained from $Z \to ee$ events, for electrons in the EM barrel calorimeter (EMB) with $|\eta| < 0.4$, and for both the High and Medium gains. Similar results are obtained over the full coverage of the EM calorimeter. The energy deposited in this cell is typically about $(20–50)\%$ of the total energy of the electron. Included in the figure are the results of fitting the time resolution results to the expected form of $\sigma(t) = p_0/E \oplus p_1$, with fit parameters p_0 (p_1) measured in units of GeV·ns (ns). The time resolution includes a contribution of ≈ 220 ps, which is due to the LHC bunch-spread along the beamline.

The time resolution, $\sigma(t)$, is expected to follow the form $\sigma(t) = p_0/E \oplus p_1$, where E is the cell energy, $\oplus$ indicates addition in quadrature, and the fit parameters p_0 and p_1 are the coefficients of the so-called noise term and constant term, respectively. Superimposed on Fig. 2 are the results of fits to this expected form of the time resolution function. The fits yield values of p_1, which gives the time resolution in the limit of large energy deposits, of 256 ps (299 ps) for High (Medium) gain. The somewhat worse results for Medium gain are due to limited statistics in the $W \to e\nu$ sample used to determine the time calibration constants. The time resolution includes a contribution of ≈ 220 ps, which is caused by the time spread in pp collisions for a given PV position due to the

LHC bunch-spread along the beamline. Subtracting this contribution in quadrature implies the LAr contributions to the time resolution are ≈ 130 ps (≈ 200 ps) for High (Medium) gain.

The time resolution is not modeled properly in the MC simulation of the ATLAS detector and it is necessary to apply additional smearing to the MC events in order to match the time performance observed in data. To smear the MC events, the fits to the time resolution determined from $Z \to ee$ data as a function of the energy of the most energetic cell in the second layer are used. The fits are parameterized in terms of the pseudorapidity of the cell and the gain scale used to reconstruct the time. To account for the impact of the beam-spread, the smearing includes a component with a Gaussian standard deviation of 220 ps that is applied in a correlated way to all photons in the same event. In addition, an uncorrelated component is applied separately to each photon to match its overall time resolution to that observed in data.

C. Measurements of delayed particles

The OFC values in Eq. 1 deviate from being optimal for signals that are early or delayed with respect to the time used to determine the OFC values. This effect can cause the reconstructed values of the energy and time to deviate from their true values.

A source of early and delayed particles can be obtained using so-called satellite bunches of protons that, due to the radio-frequency structure of the LHC accelerator and injection complex, are present in the LHC beams but separated from the main bunches by multiples of ± 5 ns. A study was made using $W \to e\nu$ and $Z \to ee$ events produced in collisions between pairs of such satellite bunches that occur at the center of the detector but are 5 ns early or late, compared to nominal collisions. These "satellite–satellite" collisions are suppressed in rate by a factor of about one million compared to collisions of the nominal bunches, since the typical population of a satellite bunch is about a factor of one thousand lower than that of the nearby nominal bunch. However, the 8 TeV data sample is sufficiently large that a statistically significant observation of these satellite–satellite collisions could be made.

The values of the mean times reconstructed for electrons produced in satellite–satellite collisions were determined to be ≈ -5.1 ns ($\approx +5.4$ ns), for events that occurred 5 ns early (late), demonstrating that the use of fixed OFC values causes a bias for signals that are sufficiently early or late compared to the nominal time. In contrast to the time reconstruction, the studies show that the reconstructed energies are very insensitive to modest time shifts of the samples on the waveform, as expected due to the methods used to calculate the OFC values used in the energy calculation. For time shifts within ± 5 ns of the nominal time, the reconstructed energy decreases by less than 1%.

III. DATA AND MONTE CARLO SIMULATION SAMPLES

This analysis uses the full dataset of pp collision events at a center-of-mass energy of $\sqrt{s} = 8$ TeV, recorded with the ATLAS detector in 2012. The data sample, after applying quality criteria that require all ATLAS sub-detector systems to be functioning normally, corresponds to a total integrated luminosity of 20.3 fb^{-1}.

While all background studies, apart from some cross-checks, are performed with data, MC simulations are used to study the response to GMSB signal models, as a function of the free parameters Λ and τ. The other GMSB parameters are fixed to the following SPS8 model values: the messenger mass $M_{\mathrm{mess}} = 2\Lambda$, the number of SU(5) messengers $N_5 = 1$, the ratio of the vacuum expectation values of the two Higgs doublets $\tan\beta = 15$, and the Higgs-sector mixing parameter $\mu > 0$ [29].

The full GMSB SPS8 SUSY mass spectra, branching fractions and decay widths are calculated from this set of parameters using ISAJET [36] version 7.80. The HERWIG++ generator, version 2.4.2 [37], was used to generate the signal MC samples, with MRST 2007 LO* [38] parton density distributions (PDF). A total of 30 signal points, from $\Lambda = 70$ TeV to $\Lambda = 400$ TeV, were generated, with τ values of 2 ns or 6 ns. For each signal point, 40,000 inclusive GMSB SUSY events were simulated. For each sample, the NLSP was forced to decay to a photon and gravitino, with the branching fraction $BR(\tilde{\chi}_1^0 \to \gamma\tilde{G})$ fixed to unity. Other τ values were simulated by appropriately reweighting the events of these generated samples, with weights related to the decay times of the neutralinos, to mimic the expected decay time distributions.

Signal cross sections are calculated to next-to-leading order (NLO) in the strong coupling constant using PROSPINO2 [39][2]. The nominal cross section and its uncertainty are taken from an envelope of cross-section predictions using different PDF sets and factorization and renormalization scales, as described in Ref. [44]. Uncertainties on the cross-section values range from 9% to 14%.

All MC samples used in this analysis were passed through a GEANT4-based simulation [45, 46] of the ATLAS detector and were reconstructed with the same algorithms used for the data. The effect of multiple pp interactions in the same or nearby bunch crossings (pileup) is taken into account in all MC simulations and the distribution of the number of interactions per bunch crossing in the MC simulation is reweighted to that observed in the data. During the 2012 data-taking period, the average number of pp collisions per bunch crossing varied between 6 and 40, with a mean value of 20.7,

---

[2] In addition a resummation of soft gluon emission at next-to-leading-logarithm accuracy (NLL) [39–43] is performed in the case of strong SUSY pair production.

IV. OBJECT RECONSTRUCTION AND IDENTIFICATION

The reconstruction and identification of electrons and photons are described in Refs. [47, 48] and [49], respectively. The photon identification criteria described in Ref. [49] have been re-optimized for the expected pileup conditions of the 8 TeV run period. Shape variables computed from the lateral and longitudinal energy profiles of the EM showers in the calorimeter are used to identify photons and discriminate against backgrounds. A set of photon selection criteria, designed for high efficiency and modest background rejection, defines the so-called "*loose*" photon identification used in this analysis. The loose photon requirements use variables that describe the shower shape in the second layer of the EM calorimeter and leakage into the hadronic calorimeter. These selection criteria do not depend on the transverse energy of the photon (E_T), but do vary as a function of η in order to take into account variations in the calorimeter geometry and upstream material. The efficiency of these loose requirements, for the signal photons, is over 95% over the range $|z_{\text{origin}}| < 250$ mm and steadily falls to approximately 75% at $|z_{\text{origin}}| = 700$ mm.

The measurement of E_T^{miss} [50] is based on the energy deposits in the calorimeter with $|\eta| < 4.9$ and the energy associated with reconstructed muons; the latter is estimated using the momentum measurement of its reconstructed track. The energy deposits associated with reconstructed objects (jets defined using the anti-k_t algorithm [51] with radius parameter 0.4, photons, electrons) are calibrated accordingly. Energy deposits not associated with a reconstructed object are calibrated according to their energy sharing between the EM and hadronic calorimeters.

V. EVENT SELECTION

The selected events were collected by an online trigger requiring the presence of at least two loose photons with $|\eta| < 2.5$, one with $E_T > 35$ GeV and the other with $E_T > 25$ GeV. This trigger is insensitive to the time of arrival of photons that are relevant for the signal considered, but there may be a slight dependence of the trigger efficiency on the z_{origin} of the photon. This effect is discussed in Sec. VIII A. The trigger efficiency exceeds 99% for signal events that pass the offline selection cuts. To ensure the selected events resulted from a *pp* collision, events are required to have at least one PV candidate with five or more associated tracks, each with transverse momentum satisfying $p_T > 400$ MeV. In case of multiple vertices, the PV is chosen as the vertex with the greatest sum of the squares of the transverse momenta of all associated tracks.

The offline photon selection requires two loose photons with $E_T > 50$ GeV and $|\eta| < 2.37$ (excluding the transition region between the barrel and endcap EM calorimeter at $1.37 < |\eta| < 1.52$). At least one photon is required to be in the barrel region $|\eta| < 1.37$. Both photons are required to be isolated, by requiring that the transverse energy deposited in the calorimeter in a cone of radius $\Delta R = \sqrt{(\Delta\eta)^2 + (\Delta\phi)^2} = 0.4$ around each photon candidate be less than 4 GeV, after corrections to account for pileup and the energy deposition from the photon itself [49]. To avoid collisions due to satellite bunches, both photons are required to have a time that satisfies $|t_\gamma| < 4$ ns.

The selected diphoton sample is divided into exclusive subsamples according to the value of E_T^{miss}. The subsample with $E_T^{\text{miss}} < 20$ GeV is used to model the prompt backgrounds, as described in Sec. VI B. The events with $20 \text{ GeV} < E_T^{\text{miss}} < 75$ GeV are used as control samples to validate the analysis procedure and background model. Diphoton events with $E_T^{\text{miss}} > 75$ GeV define the signal region.

Table I summarizes the total acceptance times efficiency of the selection requirements for examples of GMSB SPS8 signal model points with various Λ and τ values. Strong SUSY pair production is only significant for $\Lambda < 100$ TeV. For $\Lambda = 80$ TeV and $\tau = 6$ ns, the acceptance times efficiency is evaluated from MC samples to be $1.6 \pm 0.1\%$ and $2.1 \pm 0.1\%$ for weak and strong production, respectively, corresponding to a total value of $1.7 \pm 0.1\%$. For fixed Λ, the acceptance falls approximately exponentially with increasing τ, dominated by the requirement that both NLSP decay before reaching the EM calorimeter, so that the resulting photons are detected. For fixed τ, the acceptance increases with increasing Λ, since the SUSY particle masses increase, leading the decay cascades to produce, on average, higher E_T^{miss} and also higher E_T values of the decay photons.

TABLE I. The total signal acceptance times efficiency, given in percent, of the event selection requirements, for sample GMSB SPS8 model points with various Λ and τ values. The uncertainties shown are statistical only.

τ	Signal acceptance times efficiency [%]		
[ns]	$\Lambda = 80$ TeV	$\Lambda = 160$ TeV	$\Lambda = 320$ TeV
0.5	8.4 ± 0.6	30 ± 1	46 ± 2
2	5.1 ± 0.3	21 ± 0.2	33.0 ± 0.3
6	1.7 ± 0.1	7.3 ± 0.1	12.5 ± 0.2
10	0.86 ± 0.03	3.71 ± 0.06	6.45 ± 0.09
40	0.089 ± 0.004	0.38 ± 0.01	0.70 ± 0.02
100	0.016 ± 0.001	0.070 ± 0.002	0.129 ± 0.004

VI. SIGNAL AND BACKGROUND MODELING

The analysis exploits both the pointing and time measurements. However, the measured properties of only one of the two photons are used, where the choice of which

photon to use is made according to the location of the two photons. The selection requires at least one of the photons to be in the barrel region, since events with both photons in the endcap calorimeters are expected to contribute very little to the signal sensitivity. For events, referred to hereafter as BE events, where one photon is found in the barrel and one in the endcap calorimeter, the Δz_γ and t_γ measurements of the barrel photon are used in the analysis; this choice is made since, due to geometry, the Δz_γ resolution in the barrel calorimeter is better. For so-called BB events, with both photons in the EM barrel calorimeter, the Δz_γ and t_γ measurements of the photon with the maximum value of t_γ are used. Studies showed that this approach achieves a sensitivity very similar to that when using both photons, while avoiding the complexity of having to deal with the correlations between the measurements of the two photons within a single event.

A. GMSB SPS8 signal

The shape of the Δz_γ and t_γ distributions for signal events is obtained from the signal MC samples. For a given value of Λ, the distributions for any NLSP lifetime value can be obtained by appropriately reweighting the distributions of the existing MC samples.

Examples of Δz_γ and t_γ signal distributions for a few representative GMSB SPS8 models are shown in Fig. 3. The distributions are normalized to unity area within the displayed horizontal-axis range, in order to allow for an easier comparison between the various signal and background shapes. The upper two plots show signal shapes for some example NLSP lifetime (τ) values, all with Λ fixed to a value of 160 TeV. The lower two plots show signal shapes for some example Λ values, all with τ fixed to a value of 1 ns. The signal shapes have some dependence on Λ due to its impact on the SUSY mass spectrum, and therefore the event kinematics. However, the signal shapes vary most strongly with NLSP lifetime. For larger τ values, the signal shapes are significantly impacted by the diphoton event selection, which effectively requires that both NLSP decay before reaching the EM calorimeters, leading to a signal acceptance that falls rapidly with increasing time values. As a result, the signal shapes for τ values of 2.5 ns and 25 ns, for example, are quite similar, as shown in the upper plots of Fig. 3.

B. Backgrounds

The background is expected to be completely dominated by pp collision events, with possible backgrounds due to cosmic rays, beam-halo events, or other noncollision processes being negligible. The source of the loose photons in background events contributing to the selected sample is expected to be either a prompt photon, an electron misidentified as a photon, or a jet misidenti-

fied as a photon. In each case, the object providing the loose photon signature originates from the PV.

The pointing and time distributions expected for the background sources are determined using control samples in data. In addition to avoiding a reliance on the precise MC simulation of the pointing and timing performance for the backgrounds, and particularly of the tails of their Δz_γ and t_γ distributions, using data samples naturally accounts for the influence of pile-up, the possibility of selecting the wrong PV, and any instrumental or other effects that might influence the background measurements.

Given their similar EM shower developments, the pointing and time resolutions for prompt photons are similar to those for electrons. The t_γ distribution in each Δz_γ category is modeled using electrons from $Z \to ee$ data events. The $Z \to ee$ event selection requires a pair of oppositely charged electron candidates, each of which has $p_T > 35$ GeV and $|\eta| < 2.37$ (excluding the transition region between the barrel and endcap calorimeters). Both electrons are required to be isolated, with the transverse energy deposited in the calorimeter in a cone of size $\Delta R = 0.2$ around each electron candidate being less than 5 GeV, after subtracting the energy associated with the electron itself. As for photons, electrons must be read out using either High or Medium gain, and must have a time less than 4 ns. The dielectron invariant mass is required to be within 10 GeV of the Z boson mass, yielding a sufficiently clean sample of $Z \to ee$ events. The electrons are used to construct Δz_γ and t_γ templates. The unit-normalized $Z \to ee$ templates are shown superimposed on the plots of Fig. 3.

Due to their wider showers in the EM calorimeter, jets have a wider Δz_γ distribution than prompt photons and electrons. Events passing the diphoton selection with $E_T^{miss} < 20$ GeV are used as a data control sample that includes jets with properties similar to the background contributions expected in the signal region. The E_T^{miss} requirement serves to render negligible any possible signal contribution in this control sample. The time resolution depends on the deposited energy in the calorimeter. Using the shape of the $E_T^{miss} < 20$ GeV template to describe events in the signal region, defined with $E_T^{miss} > 75$ GeV therefore implicitly relies on the kinematic distributions for photons in both regions being similar. However, it is expected that there should be a correlation between the value of E_T^{miss} in a given event, and the E_T distribution of the physics objects in that event. This correlation is indeed observed in the low-E_T^{miss} control region samples. Increasing to 60 GeV the minimum E_T requirement on the photons in the $E_T^{miss} < 20$ GeV control sample selects photons with similar kinematic properties to the photons in the signal region. Therefore, the $E_T^{miss} < 20$ GeV sample requiring $E_T > 60$ GeV for the photons is used to model the background.

The selected diphoton sample with $E_T^{miss} < 20$ GeV should be dominated by jet–jet, jet–γ and $\gamma\gamma$ events. Therefore, the associated Δz_γ and t_γ distributions in-
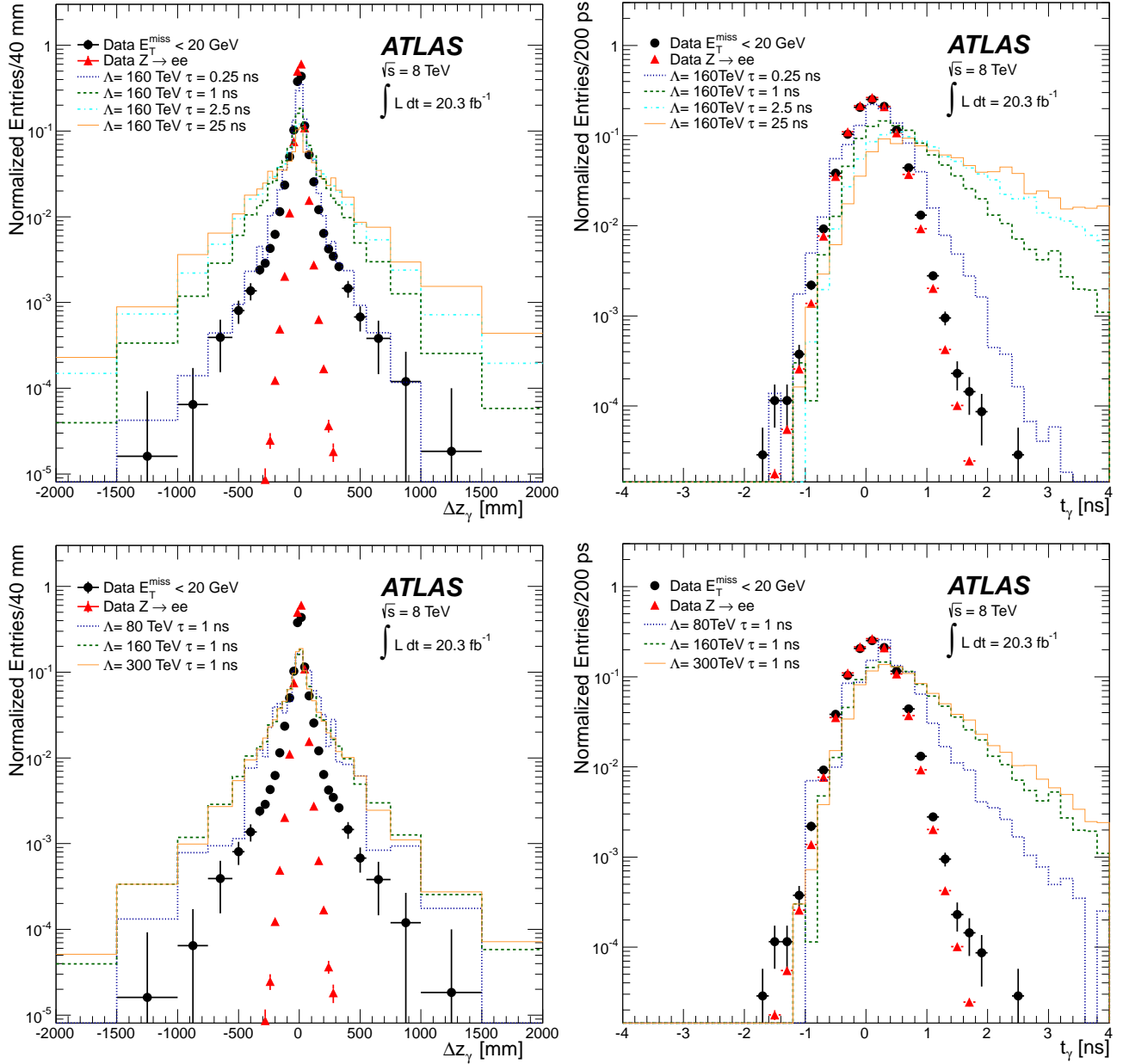
FIG. 3. Signal distributions for (left) Δz_γ and (right) t_γ, for some example GMSB SPS8 model points. The upper two plots show signal shapes for NLSP lifetime (τ) values of 0.25, 1, 2.5, and 25 ns, all with the effective scale of SUSY breaking (Λ) fixed to a value of 160 TeV. The lower two plots show signal shapes for Λ values of 80, 160, and 300 TeV, all with τ fixed to a value of 1 ns. Superimposed on each of the plots are the corresponding data distributions for the samples used to model the backgrounds, namely $Z \to ee$ events and diphoton events with $E_T^{\mathrm{miss}} < 20$ GeV. For all plots, the distributions are normalized to unity area within the horizontal-axis range displayed, and the uncertainties shown on the data distributions are statistical only.

clude contributions from photons as well as from misidentified jets that satisfy the loose photon signature. The unit-normalized $E_T^{\mathrm{miss}} < 20$ GeV templates are shown superimposed on the plots of Fig. 3. As expected, Fig. 3 shows that the Δz_γ distribution is much wider for the $E_T^{\mathrm{miss}} < 20$ GeV sample than for the $Z \to ee$ sample, while the t_γ distributions of these two background samples are very similar. Both backgrounds have distri-

butions that are very different than those expected for GMSB SPS8 signal events, with larger differences observed for higher lifetime values.

VII.   STATISTICAL ANALYSIS

The photon pointing and time measurements are each sensitive to the possible presence of photons from displaced decays of heavy, long-lived NLSP. In addition, the measurements of Δz_γ and t_γ are almost completely uncorrelated for prompt backgrounds. The lack of correlation results from the fact that Δz_γ uses the spread of the EM shower to precisely measure its centroids in the first two layers in the EM calorimeter, while t_γ uses the time reconstructed from the pulse-shape of only the second-layer cell with the maximum energy deposit. Using both variables to distinguish signal from background is therefore a powerful tool.

Since the Δz_γ distribution should be symmetric for both signal and background, the pointing distribution is folded by taking $|\Delta z_\gamma|$ as the variable of interest instead of Δz_γ. The inputs to the statistical analysis are, therefore, the values of $|\Delta z_\gamma|$ and t_γ measured for the photon selected in each event.

A full two-dimensional (2D) analysis of $|\Delta z_\gamma|$ versus t_γ would require populating a very large number of bins of the corresponding 2D space with both the background and signal models. Since the background model is determined using data in control samples, which have limited numbers of events, this approach is impractical. Instead, the original 2D analysis is transformed into a "N × 1D" problem by using the $|\Delta z_\gamma|$ values to define N mutually exclusive categories of photons, and then simultaneously fitting the t_γ spectra of each of the categories. To optimize the sensitivity of the analysis, the categories are chosen to divide the total sample of photons into categories with different signal-to-background ratios. This approach is similar to that followed in the ATLAS determination of the Higgs boson spin in the $H \rightarrow \gamma\gamma$ decay channel [52].

An additional motivation for applying the "N × 1D" approach is to simplify the task of modeling the overall background with an unknown mixture of the background templates measured using the $Z \rightarrow ee$ and $E_{\rm T}^{\rm miss} < 20$ GeV samples. As shown in Fig. 3, these samples used to model the various background contributions have different $|\Delta z_\gamma|$ distributions, but very similar t_γ distributions. The minor t_γ differences can be handled, as described in Sec. VIII, by including a small systematic uncertainty on the t_γ background shape. However, the $|\Delta z_\gamma|$ distribution of the total background depends sensitively on the background composition. By implementing the normalization of the background in each $|\Delta z_\gamma|$ category as an independent, unconstrained nuisance parameter, the fitting procedure eliminates the need to predict the overall $|\Delta z_\gamma|$ distribution of the total background, thereby avoiding the associated dependence on knowledge of the background composition.

The binning in both $|\Delta z_\gamma|$ and t_γ was chosen to optimize the expected sensitivity. It was found that using six $|\Delta z_\gamma|$ categories and six t_γ bins provides the analysis with good expected sensitivity, without undue complexity. While the optimized choice of bin boundaries has almost no dependence on Λ, there is some dependence on NLSP lifetime. The analysis, therefore, uses two separate choices of binning, one for low lifetime values ($\tau < 4$ ns) and one for high lifetime values ($\tau > 4$ ns). The optimized category and bin boundaries for both cases are summarized in Tables II and III, respectively.

The one-dimensional fits of the t_γ distributions of the individual categories are performed simultaneously. The signal normalization is represented by a single unconstrained signal-strength parameter, μ, that is correlated between all categories and defined as the fitted signal cross section divided by the GMSB SPS8 prediction. Thus, there are seven unconstrained parameters in the fit, namely six separate nuisance parameters, one for each category, describing the background normalization, and the signal strength μ.

The analysis uses a likelihood model $\mathcal{L}(\mu, \theta)$ that is dependent on the signal strength μ and the values of the nuisance parameters θ. The model incorporates a statistical Poisson component as well as Gaussian constraint terms for the nuisance parameters associated with systematic uncertainties. The statistical model and procedure are implemented within the HistFactory framework [53]. Two likelihood-based test statistics q_0 and q_μ are calculated to find the p_0 values for the background-only hypothesis and to set upper limits on the signal strength.

Asymptotic formulae based on Wilk's theorem are used to approximate the q_0 and q_μ distributions following the procedures documented in Ref. [54]. Tests of the background model's validity in the control regions and the signal region rely on the p_0 test statistic, calculated from the observed q_0. In the absence of any excess, the CL_S exclusions for each signal type are calculated according to Ref. [55].

To validate the statistical model and asymptotic forms of q_0 and q_μ, unconditional pseudo-experiment ensembles were generated from the background-only model and multiple signal-plus-background models. Although the number of data events in the signal region is not large, deviations from the asymptotic χ^2 distribution of q_μ were shown to have a minimal impact on the exclusion. The model accurately reconstructed the signal and background normalization parameters and produced Gaussian distributions of the constrained nuisance parameters.

VIII.   SYSTEMATIC UNCERTAINTIES

In the statistical analysis, the background normalization for each $|\Delta z_\gamma|$ category is determined using an independent nuisance parameter. Therefore, it is not necessary to include systematic uncertainties regarding the normalization of the background, nor regarding its shape in the variable $|\Delta z_\gamma|$. As a result, the various systematic uncertainties relevant for this analysis can be divided

TABLE II. Values of the optimized ranges of the six $|\Delta z_\gamma|$ categories, for both low and high NLSP lifetime (τ) values.

NLSP	Range of $|\Delta z_\gamma|$ values for each category [mm]					
Lifetime	Cat. 1	Cat. 2	Cat. 3	Cat. 4	Cat. 5	Cat. 6
$\tau < 4$ ns	$0-40$	$40-80$	$80-120$	$120-160$	$160-200$	$200-2000$
$\tau > 4$ ns	$0-50$	$50-100$	$100-150$	$150-200$	$200-250$	$250-2000$

TABLE III. Values of the optimized ranges of the six t_γ bins, for both low and high NLSP lifetime (τ) values.

NLSP	Range of t_γ values for each bin [ns]					
Lifetime	Bin 1	Bin 2	Bin 3	Bin 4	Bin 5	Bin 6
$\tau < 4$ ns	$-4.0-+0.5$	$0.5-1.1$	$1.1-1.3$	$1.3-1.5$	$1.5-1.8$	$1.8-4.0$
$\tau > 4$ ns	$-4.0-+0.4$	$0.4-1.2$	$1.2-1.4$	$1.4-1.6$	$1.6-1.9$	$1.9-4.0$

into two categories: so-called "flat" uncertainties are not a function of $|\Delta z_\gamma|$ and t_γ and affect only the overall signal yield, while "shape" uncertainties are those that are related to the shapes of the unit-normalized $|\Delta z_\gamma|$ and t_γ distributions for signal or to the shape of the background t_γ template.

A. Signal yield systematic uncertainties

The various flat systematic uncertainties affecting the signal yield are summarized in Table IV. The uncertainty on the integrated luminosity is $\pm 2.8\%$ and is determined with the methodology detailed in Ref. [56]. The uncertainty due to the trigger is dominated by uncertainties on the dependence on $|\Delta z_\gamma|$ of the efficiency of the hardware-based Level 1 (L1) trigger. The L1 calorimeter trigger [57] uses analog sums of the channels grouped within projective trigger towers. This architecture leads to a small decrease in L1 trigger efficiency for highly nonpointing photons, due to energy leakage from the relevant trigger towers. The uncertainty on the impact of this dependence is conservatively set to the magnitude of the observed change in efficiency in signal MC events versus $|\Delta z_\gamma|$, and dominates the $\pm 2\%$ uncertainty on the trigger efficiency.

Following the method outlined in Ref. [58], uncertainties on the signal efficiency, arising from the combined impact of uncertainties in the photon energy scale and resolution and in the combined photon identification and isolation efficiencies, are determined to be $\pm 1\%$ and $\pm 1.5\%$, respectively. An additional 4% is included as a conservative estimate of the uncertainty in the identification efficiency due to the non-pointing nature of the photons. This estimate is derived from studies of changes in the relevant variables measuring the shapes of the EM showers for non-pointing photons. An uncertainty on the signal yield of $\pm 1.1\%$ results from varying the E_T^{miss} energy scale and resolution within their estimated uncertainties [50]. The uncertainty on the signal efficiency due to MC statistics lies in the range $\pm (0.8-3.6)\%$ and the contribution due to the lifetime reweighting technique is in the range

$\pm (0.5-5)\%$, depending on the sample lifetime.

Variations in the calculated NLO signal cross sections times the signal acceptance and efficiency, at the level of $\pm (9-14)\%$ occur when varying the PDF set and factorization and renormalization scales, as described in Sec. III. In the results, these uncertainties on the theoretical cross section are shown separately, as hashed bands around the theory prediction. Limits are quoted at the points where the experimental results equal the value of the central theory prediction minus one standard deviation of the theoretical uncertainty.

TABLE IV. Summary of relative systematic uncertainties that affect the normalization of the signal yield. The last row summarizes the relative uncertainty on the theoretical cross section, and is treated separately, as explained in the text.

Source of uncertainty	Value [%]
Integrated luminosity	± 2.8
Trigger efficiency	± 2
Photon E_T scale/resolution	± 1
Photon identification and isolation	± 1.5
Non-pointing photon identification	± 4
E_T^{miss} reconstruction	± 1.1
Signal MC statistics	$\pm (0.8-3.6)$
Signal reweighting	$\pm (0.5-5)$
Signal PDF and scale uncertainties	$\pm (9-14)$

B. Signal shape systematic uncertainties

The expected signal distributions are determined using the GMSB SPS8 MC signal events. Therefore, limitations in the MC simulation could lead to differences between data and MC events in the predicted signal behavior. Any such discrepancies in the shapes of the signal distributions must be handled by corresponding systematic uncertainties on the signal shapes. Since signal templates for both $|\Delta z_\gamma|$ and t_γ are used in the statistical

analysis, systematic uncertainties on the signal shapes of both must be taken into account in the fitting procedure.

The dominant systematic uncertainty on the shape of the signal t_γ distribution arises from the impact of the time reconstruction algorithm on the measurement of delayed signals. As discussed in Sec. II C, the use of fixed OFC values causes a bias in the energy and time reconstructed for signals that are sufficiently early or late compared to the nominal time. For time shifts within ± 5 ns of the nominal time, the reconstructed energy decreases by less than 1% and, as a result, impacts on the measurements of the photon energy and pointing are negligible. However, for time shifts of ± 5 ns, a bias in the time reconstruction of order 10% of the shift is observed in the analysis of satellite–satellite collisions. Since the optimal filtering approach is equivalent to a linearization of the optimization problem, the expected form of the time bias is expected to be dominated by the neglected quadratic terms in the Taylor expansion. Therefore, one expects deviations in the time measurement to be small for small time shifts, over a region where the linear approximation works well, and then to grow roughly quadratically for larger time shifts. As a conservative estimate of the systematic uncertainty on the time measurement due to these effects, a linear dependence is assumed for the deviations, with an amplitude of $\pm 10\%$ of the reconstructed time. This uncertainty is applied only to the signal time distribution, since the background time shape is determined directly from data and therefore already includes whatever impact is caused by the bias.

Another source of systematic uncertainty in the signal $|\Delta z_\gamma|$ and t_γ shapes results from possible differences between the pileup conditions in data and signal MC events, even though the MC signal samples are reweighted to match the pileup distribution observed in the data. The PV in GMSB SPS8 signal events should be correctly identified with high efficiency, typically greater than 90%, due to the high E_T values of the other SM particles produced in the SUSY decay chains. However, the presence of pileup could still increase the likelihood of incorrectly choosing the PV, potentially impacting both the pointing and time measurements. Nearby energy deposits that are not associated with the photon could also impact the photon measurements, though these should be moderated by the photon isolation requirements. As a conservative estimate of the possible influence of pileup, the signal shapes in the entire MC sample were compared with those in two roughly equally sized subsamples with differing levels of pileup, chosen as those events with less than, and those with greater than or equal to, 13 reconstructed PV candidates. The small differences observed are included as pileup-induced systematic uncertainties on the signal template shapes.

To investigate the possible impact of the imperfect knowledge of the material distribution in front of the calorimeter, one signal MC point was simulated with the nominal detector description as well as with a modified version that varies the material description within the un-

certainties. The signal distributions using the two detector geometries are very similar, typically agreeing within a few percent. These variations are small compared to the other systematic uncertainties on the signal shapes, and are therefore neglected.

Typical values of the total systematic uncertainties on the signal shapes are around $\pm 10\%$, dominated by the impact of the time reconstruction algorithm on the measurement of delayed signals. These uncertainties have a very small impact on the overall sensitivity of the analysis, which is dominated by statistical uncertainties due to the limited size of the data sample in the signal region.

C. Background shape systematic uncertainties

The dominant uncertainty in the knowledge of the background template shape arises from uncertainty in the background composition in the signal region. As described in Sec. VI B, and seen in Fig. 3, the EM shower development of electrons and photons differs from that of jets and gives rise to somewhat different t_γ shapes, and very different $|\Delta z_\gamma|$ shapes. Therefore, the t_γ and $|\Delta z_\gamma|$ shapes for the total background depend on the background composition.

The statistical analysis includes an independent normalization fit parameter for the total background in each of the $|\Delta z_\gamma|$ categories. By this means, the fit result avoids any dependence on the $|\Delta z_\gamma|$ distribution of the background and it is not necessary to account for systematic uncertainties on the background $|\Delta z_\gamma|$ shape. However, the background t_γ shape is used in the fitting procedure, and therefore its associated systematic uncertainties must be taken into account.

Since the time measurement is performed using only the second-layer cell of the EM cluster with the maximum energy deposit, it is expected that the time should be rather insensitive to the details of the EM shower development and, therefore, one would expect very similar time distributions for prompt electrons, photons and jets. As seen in Fig. 3, this expectation is largely satisfied since the $Z \to ee$ and $E_T^{\mathrm{miss}} < 20$ GeV t_γ distributions are indeed very similar. However, there are some effects that could cause a slight violation of the assumption that the t_γ distribution would be the same for all prompt background sources. Details of the EM shower development can indirectly impact the time measurement, for example, due to cross-talk from neighboring cells. In addition, the time measurement necessarily includes a correction for the time of flight from the PV; therefore, misidentification of the PV can lead to shifts in the reconstructed time away from the true time, and different background sources can have different rates of PV misidentification. PV misidentification can also produce shifts in the pointing measurement, introducing a non-zero correlation between t_γ and $|\Delta z_\gamma|$, even for prompt backgrounds.

The t_γ template from the diphoton sample with $E_T^{\mathrm{miss}} < 20$ GeV includes contributions from jets as well

as EM objects and is taken as the nominal estimate of the background t_γ shape. The difference between this distribution and that of the $Z \to ee$ sample, which has a higher purity of EM objects, is taken as an estimate of the uncertainty due to the background composition and is symmetrized to provide a symmetric systematic uncertainty on the background t_γ shape. The uncertainty is small for low time values, but reaches almost $\pm100\%$ in the highest t_γ bin. However, this uncertainty has little impact on the overall sensitivity since the signal yield in the highest t_γ bin is much larger than the background expectation, even when this large background uncertainty is taken into account.

Another uncertainty in the background t_γ shape arises from uncertainties in the relative contributions of BB and BE events to the background in the signal region. The definition of t_γ for BB events as the time of the photon with the maximum time value produces, as mentioned previously, a small shift toward positive time values for such events, which does not exist for BE events. Therefore, in constructing the total background t_γ template, it is necessary to appropriately weight the t_γ background templates measured separately for BB and BE events in order to match the background in the signal region. Since any signal can have a different BB/BE composition than the background, the rate of BB and BE events in the signal region cannot simply be used to determine the background composition. However, the background-dominated control regions can be used to make an estimation of the background BB/BE composition. Comparing the various samples with $E_T^{\text{miss}} < 75$ GeV, BB events are estimated to contribute $(61 \pm 4)\%$ of the total background in the signal region, where the uncertainty conservatively covers the variations observed among various samples. Therefore, the nominal t_γ background template is formed by appropriately weighting the BB and BE background distributions to this fraction, with BB fractions varied by $\pm4\%$ to generate the $\pm1\sigma$ variations on this shape due to the uncertainty in the BB/BE background contributions. This systematic shape uncertainty reaches less than $\pm10\%$ in the highest t_γ bin and, therefore, is much smaller than the dominant uncertainty due to the background composition.

An additional systematic uncertainty on the background t_γ shape arises from the event kinematics. As discussed in Sec. VI B, the minimum E_T requirements on the photons are increased to 60 GeV for the $E_T^{\text{miss}} < 20$ GeV control sample, as opposed to 50 GeV for the signal region, in order for the $E_T^{\text{miss}} < 20$ GeV control sample to select photons with kinematic properties more similar to the background photons expected in the signal region. Systematic uncertainties on the t_γ shape of the $E_T^{\text{miss}} < 20$ GeV sample are determined by varying the photon E_T requirement up and down by 10 GeV. The three shapes agree quite well with each other, with the observed variations reaching about $\pm40\%$ in the highest time bin.

IX. RESULTS AND INTERPRETATION

Before examining the $|\Delta z_\gamma|$ and t_γ distributions of the data in the signal region, the two control regions, CR1 with $20 < E_T^{\text{miss}} < 50$ GeV and CR2 with $50 < E_T^{\text{miss}} < 75$ GeV, are used to validate the analysis technique and background modeling. Since the control regions should be dominated by background, their data distributions are expected to be well described by the background-only fit.

Table V summarizes the number of selected events in CR1 and CR2, as well as those in the signal region (SR), showing that the control region datasets are much larger than that of the signal region. It is of interest whether the background modeling, including the assigned systematic uncertainties, is adequate to describe the control region data within the statistical uncertainties of the data in the signal region. Therefore, the fitting procedure was applied separately to the measured data distributions in CR1 and CR2, scaled in each case to the total of 386 events of the signal region. The fit results for both control regions are in good agreement with the background-only model for all tested signal points, validating the analysis methodology.

TABLE V. Numbers of selected events in the two control regions (CR1 and CR2) and in the signal region (SR).

Sample	E_T^{miss} range [GeV]	Number of events
CR1	$20 < E_T^{\text{miss}} < 50$	50751
CR2	$50 < E_T^{\text{miss}} < 75$	3591
SR	$E_T^{\text{miss}} > 75$	386

Figure 4 shows the distributions of Δz_γ and t_γ for the 386 events in the signal region. The distributions of both variables are rather narrow, as expected for background. In particular, there is no evidence for events in the tail of the t_γ distribution at positive times, as would be expected for a signal contribution due to delayed photons. The Δz_γ distribution is quite symmetric around zero, as expected for both the signal and for physics backgrounds. The $|\Delta z_\gamma|$ and t_γ distributions in the final, coarser binning are used as inputs to the final fitting procedure and statistical analysis.

Example results of fits to the signal region data are shown in Fig. 5, for the particular case of $\Lambda = 100$ TeV and $\tau = 19$ ns. The figures show the results of the signal-plus-background (with $\mu = 1$) and background-only ($\mu = 0$) fits to the six $|\Delta z_\gamma|$ categories. The signal-region data are in good agreement with the background-only model, and there is no evidence for a signal-like excess.

Fits to the data were performed for τ values exceeding 250 ps, and for the range of relevant Λ values. The smallest p_0 value of 0.21, corresponding to an equivalent Gaussian significance of 0.81σ, was found for signal model parameters of $\Lambda = 100$ TeV and $\tau = 0.25$ ns. Using ensembles of background-only pseudo-experiments, the probability of observing a p_0 value this small or smaller
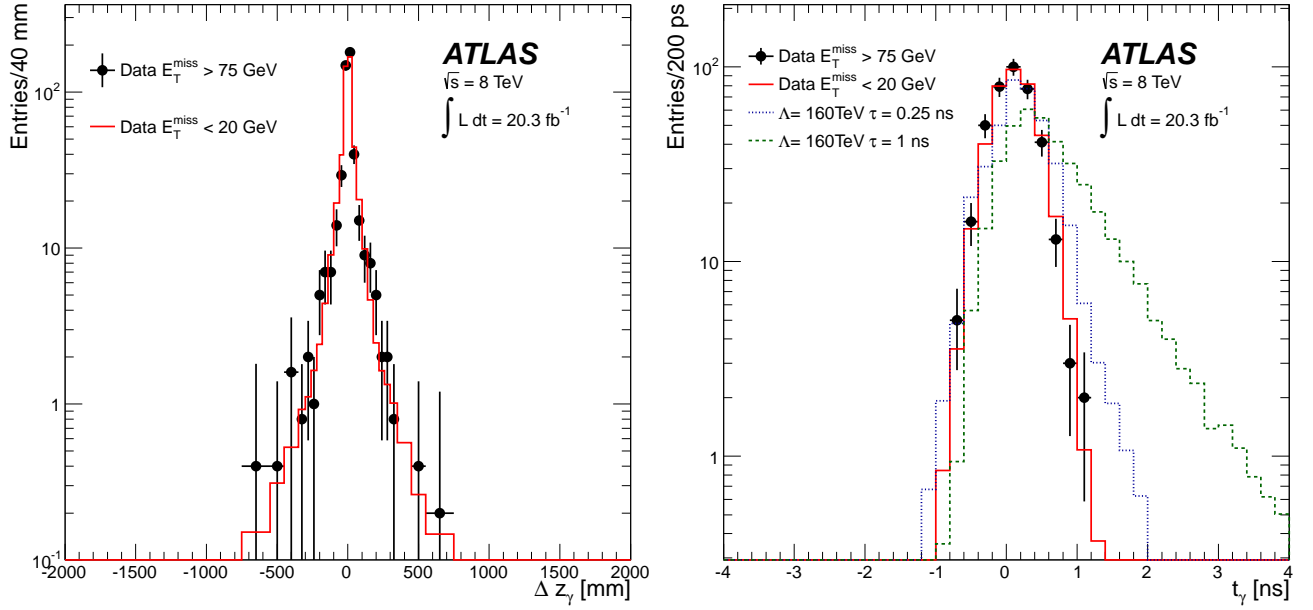
FIG. 4. Distributions of (left) Δz_γ and (right) t_γ for the 386 events in the signal region, defined with $E_T^{\mathrm{miss}} > 75$ GeV. Superimposed are the data distributions for diphoton events with $E_T^{\mathrm{miss}} < 20$ GeV, used to model the backgrounds, and the distributions for two example NLSP lifetime values in GMSB SPS8 models with $\Lambda = 160$ TeV. The background and MC signal distributions are scaled to the total number of data events in the signal region.
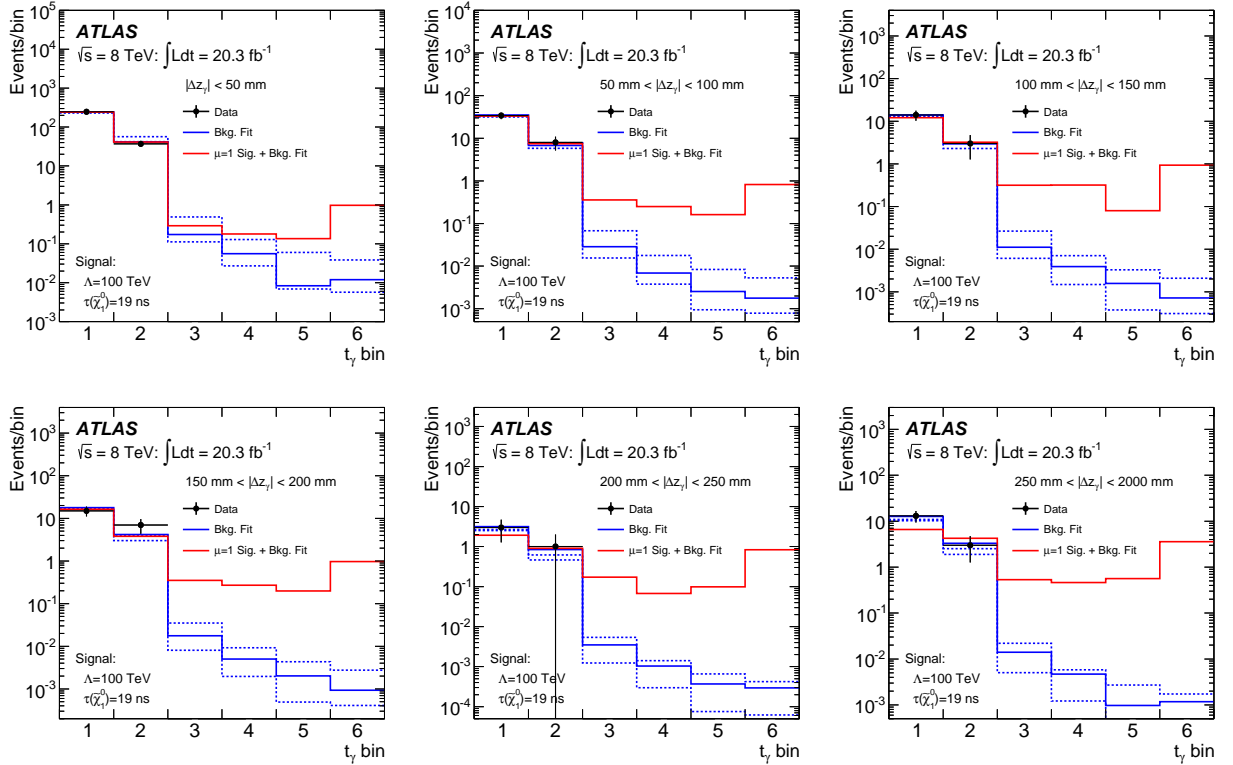

FIG. 5. Example fit to the signal-region data. The figures show the results of the signal-plus-background fits with $\mu = 1$ to the six $|\Delta z_\gamma|$ categories, along with the background-only fit and the $\pm 1\sigma$ systematic shape variations (dashed lines). The signal model shown has $\Lambda = 100$ TeV and $\tau = 19$ ns. The ranges of the t_γ bins are as defined in Table III.

from any one of the 640 signal points in the Λ–τ plane was calculated to be 88%.

Figure 6 shows, for $\Lambda = 200$ TeV, the results of the signal-region fit interpreted as 95% confidence level (CL) limits on the number of signal events, as well as on the signal cross section, as a function of $\tilde{\chi}_1^0$ lifetime (assuming the branching fraction $BR(\tilde{\chi}_1^0 \to \gamma \tilde{G}) = 1$). Each plot includes a curve indicating the GMSB SPS8 theory prediction for $\Lambda = 200$ TeV. The intersections where the limits cross the theory prediction show that, for $\Lambda = 200$ TeV, values of τ in the range between approximately 0.3 ns and 20 ns are excluded at 95% CL. The observed limits are in good agreement with the expected limits, which are also shown in Fig. 6, along with their $\pm 1\sigma$ and $\pm 2\sigma$ uncertainty bands. For large τ values, the 95% CL limits are close to the value of three events expected for a Poisson distribution with zero events observed, indicating that the results for high lifetimes are dominated by statistical uncertainties. The limits on the number of signal events are higher for low lifetimes, as it becomes more difficult to distinguish between the signal and background shapes.

By repeating the statistical procedure for various Λ and τ values, the limits are determined as a function of these GMSB SPS8 model parameters. The range of $\tilde{\chi}_1^0$ lifetimes tested is restricted to $\tau > 250$ ps to avoid the region of very low lifetimes where the shapes of the signal and background distributions become very similar. Figure 7 shows the subsequent limits in the two-dimensional GMSB signal space of $\tilde{\chi}_1^0$ lifetime versus Λ, and also versus the corresponding $\tilde{\chi}_1^0$ and $\tilde{\chi}_1^\pm$ masses in the GMSB SPS8 model. For example, $\tilde{\chi}_1^0$ lifetimes up to about 100 ns are excluded at 95% CL for Λ values in the range of about 80–100 TeV, as are Λ values up to about 300 TeV (corresponding to $\tilde{\chi}_1^0$ and $\tilde{\chi}_1^\pm$ masses of about 440 GeV and 840 GeV, respectively) for $\tilde{\chi}_1^0$ lifetimes in the range of about 2–3 ns. For comparison, the results from the ATLAS analysis of the 7 TeV dataset [1] are also shown in Fig. 7, indicating the significantly larger reach of the 8 TeV analysis.
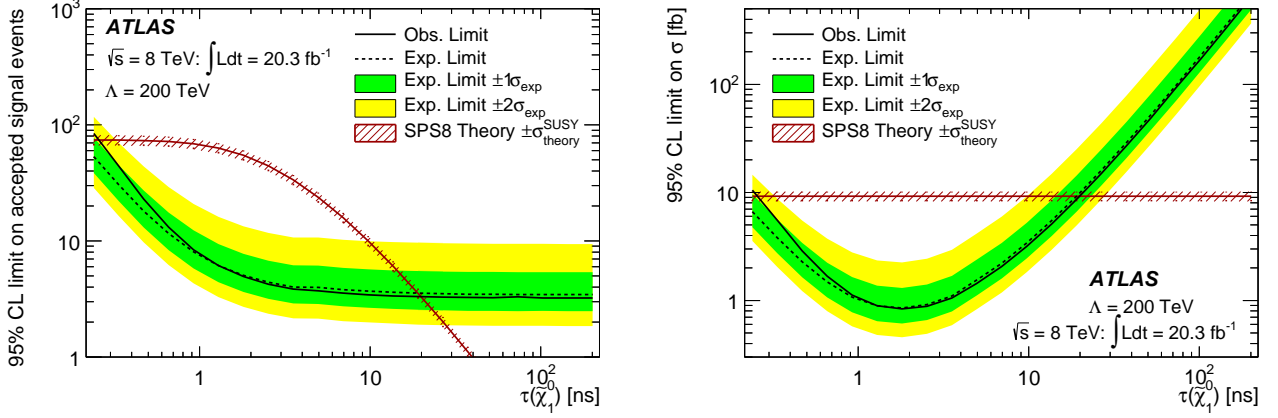
FIG. 6. The observed and expected 95% CL limits on (left) the number of signal events and (right) the GMSB SPS8 signal cross section, as a function of $\tilde{\chi}_1^0$ lifetime, for the case of $\Lambda = 200$ TeV. The regions above the limit curves are excluded at 95% CL. The red bands show the GMSB SPS8 theory prediction, including its theoretical uncertainty.
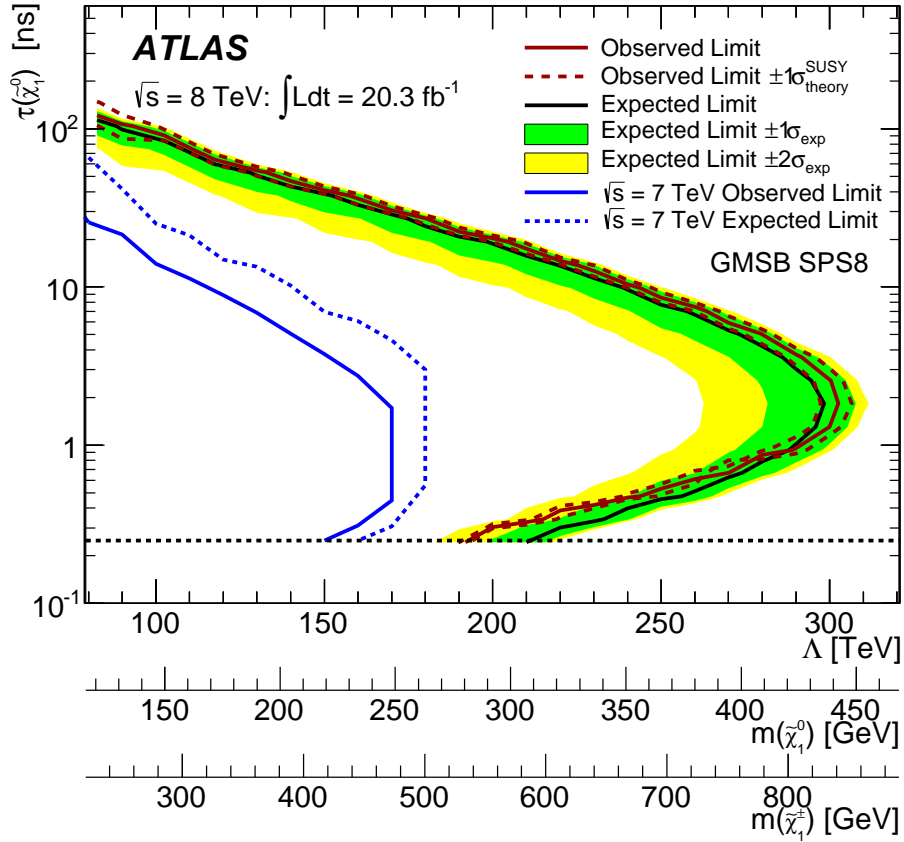
FIG. 7. The observed and expected 95% CL limits in the two-dimensional GMSB signal space of $\tilde{\chi}_1^0$ lifetime versus Λ, the effective scale of SUSY breaking, and also versus the corresponding $\tilde{\chi}_1^0$ and $\tilde{\chi}_1^\pm$ masses in the SPS8 model. For comparison, the results from the 7 TeV analysis are also shown. The regions to the left of the limit curves are excluded at 95% CL. The horizontal dashed line indicates the lowest lifetime value, namely $\tau = 250$ ps, for which the analysis is applied.

X. CONCLUSIONS

A search has been made for evidence of non-pointing and delayed photons, such as would arise in the decays of long-lived heavy neutral particles. The search, in the $\gamma\gamma + E_{\mathrm{T}}^{\mathrm{miss}} + X$ final state, uses the full data sample collected by ATLAS in 2012, corresponding to an integrated luminosity of 20.3 fb^{-1} of 8 TeV pp collisions at the LHC.

The data are in good agreement with the background-only fit and no evidence for non-pointing and delayed photons is observed. The results are interpreted in the context of the GMSB SPS8 benchmark model, in the plane of τ, the $\tilde{\chi}_1^0$ lifetime, versus Λ, the effective scale of SUSY breaking, and also versus the corresponding $\tilde{\chi}_1^0$ and $\tilde{\chi}_1^\pm$ masses. The resultant 95% CL exclusion limits include values of τ in the range from 0.25 ns to about 100 ns, and values of Λ in the range from 80 TeV to about 300 TeV.

XI. ACKNOWLEDGEMENTS

[1] ATLAS Collaboration, Phys. Rev. D **88**, 012001 (2013), `arXiv:1304.6310 [hep-ex]`.
[2] H. Miyazawa, Prog. Theor. Phys. **36 (6)**, 1266 (1966).
[3] P. Ramond, Phys. Rev. D **3**, 2415 (1971).
[4] Y. A. Golfand and E. P. Likhtman, JETP Lett. **13**, 323 (1971).
[5] A. Neveu and J. H. Schwarz, Nucl. Phys. B **31**, 86 (1971).
[6] A. Neveu and J. H. Schwarz, Phys. Rev. D **4**, 1109 (1971).
[7] J.-L. Gervais and B. Sakita, Nucl. Phys. B **34**, 632 (1971).
[8] D. V. Volkov and V. P. Akulov, Phys. Lett. B **46**, 109 (1973).
[9] J. Wess and B. Zumino, Phys. Lett. B **49**, 52 (1974).
[10] J. Wess and B. Zumino, Nucl. Phys. B **70**, 39 (1974).
[11] P. Fayet, Phys. Lett. B **64**, 159 (1976).
[12] P. Fayet, Phys. Lett. B **69**, 489 (1977).
[13] G. R. Farrar and P. Fayet, Phys. Lett. B **76**, 575 (1978).
[14] P. Fayet, Phys. Lett. B **84**, 416 (1979).
[15] S. Dimopoulos and H. Georgi, Nucl. Phys. B **193**, 150 (1981).
[16] M. Dine and W. Fischler, Phys. Lett. B **110**, 227 (1982).
[17] L. Alvarez-Gaumé, M. Claudson, and M. B. Wise, Nucl. Phys. B **207**, 96 (1982).
[18] C. R. Nappi and B. A. Ovrut, Phys. Lett. B **113**, 175 (1982).
[19] M. Dine and A. Nelson, Phys. Rev. D **48**, 1277 (1993), `hep-ph/9303230`.
[20] M. Dine, A. Nelson, and Y. Shirman, Phys. Rev. D **51**, 1362 (1995), `hep-ph/9408384`.
[21] M. Dine, A. Nelson, Y.Nir, and Y. Shirman, Phys. Rev. D **53**, 2658 (1996), `hep-ph/9507378`.
[22] ATLAS Collaboration, Phys. Lett. B **716**, 1 (2012), `arXiv:1207.7214 [hep-ex]`.
[23] CMS Collaboration, Phys. Lett. B **716**, 30 (2012), `arXiv:1207.7235 [hep-ex]`.
[24] M. Abdullah, I. Galon, Y. Shadmi, and Y. Shirman, J. High Energy Phys. 06, 057 (2013), `arXiv:1209.4904 [hep-ph]`.
[25] J. L. Evans, M. Ibe, and T. T. Yanagida, Phys.Lett. B **705**, 342 (2011), `arXiv:1107.3006 [hep-ph]`.
[26] J. L. Evans, M. Ibe, S. Shirai, and T. T. Yanagida, Phys. Rev. D **85**, 095004 (2012), `arXiv:1201.2611 [hep-ph]`.
[27] G. Giudice and R. Rattazzi, Phys. Rept. **322**, 419 (1999), `arXiv:hep-ph/9801271 [hep-ph]`.
[28] C. Chen and J. Gunion, Phys. Lett. B **420**, 77 (1998), `arXiv:hep-ph/9707302 [hep-ph]`.
[29] B. C. Allanach et al., Eur. Phys. J. C **25**, 113 (2002), `hep-ph/0202233`.
[30] CMS Collaboration, Phys. Lett. B **722**, 273 (2013), `arXiv:1212.1838 [hep-ex]`.
[31] ATLAS Collaboration, JINST **3**, S08003 (2008).
[32] N. Buchanan et al., JINST **3**, P03004 (2008).
[33] H. Abreu et al., JINST **5**, P09003 (2010).

[34] M. Aharrouche et al., Nucl. Instrum. Methods Phys. Res., Sect. A **597**, 178 (2008).

[35] W. Cleland and E. Stern, Nucl. Instrum. Methods Phys. Res., Sect. A **338**, 467 (1994).

[36] H. Baer, F. E. Paige, S. D. Protopopescu, and X. Tata, `hep-ph/0312045`.

[37] M. Bahr et al., Eur. Phys. J. C **58**, 639 (2008), `arXiv:0803.0883 [hep-ph]`.

[38] A. Sherstnev and R. S. Thorne, Eur. Phys. J. C **55**, 553 (2008), `arXiv:0711.2473 [hep-ph]`.

[39] W. Beenakker, R. Höpker, M. Spira, and P. Zerwas, Nucl. Phys. B **492**, 51 (1997), `arXiv:hep-ph/9610490 [hep-ph]`.

[40] A. Kulesza and L. Motyka, Phys. Rev. Lett. **102**, 111802 (2009), `arXiv:0807.2405 [hep-ph]`.

[41] A. Kulesza and L. Motyka, Phys. Rev. D **80**, 095004 (2009), `arXiv:0905.4749 [hep-ph]`.

[42] W. Beenakker, et al., J. High Energy Phys. 12, 041 (2009), `arXiv:0909.4418 [hep-ph]`.

[43] W. Beenakker, et al., Int. J. Mod. Phys. A **26**, 2637 (2011), `arXiv:1105.1110 [hep-ph]`.

[44] M. Krämer, et al., `arXiv:1206.2892 [hep-ph]`.

[45] GEANT4 Collaboration, S. Agostinelli et al., Nucl. Instrum. Methods Phys. Res., Sect. A **506**, 250 (2003).

[46] ATLAS Collaboration, Eur. Phys. J. C **70**, 823 (2010), `arXiv:1005.4568 [physics.ins-det]`.

[47] ATLAS Collaboration, Eur. Phys. J. **C72**, 1909 (2012), `arXiv:1110.3174 [hep-ex]`.

[48] ATLAS Collaboration, Eur. Phys. J. C **74**, 2941 (2014), `arXiv:1404.2240 [hep-ex]`.

[49] ATLAS Collaboration, Phys. Rev. D **83**, 052005 (2011), `arXiv:1012.4389 [hep-ex]`.

[50] ATLAS Collaboration, Eur. Phys. J. C **72**, 1844 (2012), `arXiv:1108.5602 [hep-ex]`.

[51] M. Cacciari, G. Salam, and G. Soyez, J. High Energy Phys. **04**, 063 (2008), `arXiv:0802.1189 [hep-ph]`.

[52] ATLAS Collaboration, Phys. Lett. B **726**, 120 (2013), `arXiv:1307.1432 [hep-ex]`.

[53] K. Cranmer, G. Lewis, L. Moneta, A. Shibata, and W. Verkerke, Tech. Rep. CERN-OPEN-2012-016, Jan, 2012. `https://cds.cern.ch/record/1456844/`.

[54] G. Cowan, K. Cranmer, E. Gross, and O. Vitells, Eur. Phys. J. C **71**, 1554 (2011), `arXiv:1007.1727 [physics.data-an]`.

[55] A. L. Read, J. Phys. G **28**, 2693 (2002).

[56] ATLAS Collaboration, Eur. Phys. J. C **73**, 2518 (2013), `arXiv:1302.4393 [hep-ex]`.

[57] R. Achenbach et al., JINST **3**, P03001 (2008).

[58] ATLAS Collaboration, Phys. Rev. D **89**, 052004 (2014), `arXiv:1311.1440 [hep-ex]`.

The ATLAS Collaboration

G. Aad[85], B. Abbott[113], J. Abdallah[152], S. Abdel Khalek[117], O. Abdinov[11], R. Aben[107], B. Abi[114], M. Abolins[90], O.S. AbouZeid[159], H. Abramowicz[154], H. Abreu[153], R. Abreu[30], Y. Abulaiti[147a,147b], B.S. Acharya[165a,165b,a], L. Adamczyk[38a], D.L. Adams[25], J. Adelman[177], S. Adomeit[100], T. Adye[131], T. Agatonovic-Jovin[13a], J.A. Aguilar-Saavedra[126a,126f], M. Agustoni[17], S.P. Ahlen[22], F. Ahmadov[65,b], G. Aielli[134a,134b], H. Akerstedt[147a,147b], T.P.A. Åkesson[81], G. Akimoto[156], A.V. Akimov[96], G.L. Alberghi[20a,20b], J. Albert[170], S. Albrand[55], M.J. Alconada Verzini[71], M. Aleksa[30], I.N. Aleksandrov[65], C. Alexa[26a], G. Alexander[154], G. Alexandre[49], T. Alexopoulos[10], M. Alhroob[113], G. Alimonti[91a], L. Alio[85], J. Alison[31], B.M.M. Allbrooke[18], L.J. Allison[72], P.P. Allport[74], A. Aloisio[104a,104b], A. Alonso[36], F. Alonso[71], C. Alpigiani[76], A. Altheimer[35], B. Alvarez Gonzalez[90], M.G. Alviggi[104a,104b], K. Amako[66], Y. Amaral Coutinho[24a], C. Amelung[23], D. Amidei[89], S.P. Amor Dos Santos[126a,126c], A. Amorim[126a,126b], S. Amoroso[48], N. Amram[154], G. Amundsen[23], C. Anastopoulos[140], L.S. Ancu[49], N. Andari[30], T. Andeen[35], C.F. Anders[58b], G. Anders[30], K.J. Anderson[31], A. Andreazza[91a,91b], V. Andrei[58a], X.S. Anduaga[71], S. Angelidakis[9], I. Angelozzi[107], P. Anger[44], A. Angerami[35], F. Anghinolfi[30], A.V. Anisenkov[109,c], N. Anjos[12], A. Annovi[47], A. Antonaki[9], M. Antonelli[47], A. Antonov[98], J. Antos[145b], F. Anulli[133a], M. Aoki[66], L. Aperio Bella[18], R. Apolle[120,d], G. Arabidze[90], I. Aracena[144], Y. Arai[66], J.P. Araque[126a], A.T.H. Arce[45], F.A. Arduh[71], J-F. Arguin[95], S. Argyropoulos[42], M. Arik[19a], A.J. Armbruster[30], O. Arnaez[30], V. Arnal[82], H. Arnold[48], M. Arratia[28], O. Arslan[21], A. Artamonov[97], G. Artoni[23], S. Asai[156], N. Asbah[42], A. Ashkenazi[154], B. Åsman[147a,147b], L. Asquith[6], K. Assamagan[25], R. Astalos[145a], M. Atkinson[166], N.B. Atlay[142], B. Auerbach[6], K. Augsten[128], M. Aurousseau[146b], G. Avolio[30], B. Axen[15], G. Azuelos[95,e], Y. Azuma[156], M.A. Baak[30], A.E. Baas[58a], C. Bacci[135a,135b], H. Bachacou[137], K. Bachas[155], M. Backes[30], M. Backhaus[30], J. Backus Mayes[144], E. Badescu[26a], P. Bagiacchi[133a,133b], P. Bagnaia[133a,133b], Y. Bai[33a], T. Bain[35], J.T. Baines[131], O.K. Baker[177], P. Balek[129], F. Balli[137], E. Banas[39], Sw. Banerjee[174], A.A.E. Bannoura[176], V. Bansal[170], H.S. Bansil[18], L. Barak[173], S.P. Baranov[96], E.L. Barberio[88], D. Barberis[50a,50b], M. Barbero[85], T. Barillari[101], M. Barisonzi[176], T. Barklow[144], N. Barlow[28], S.L. Barnes[84], B.M. Barnett[131], R.M. Barnett[15], Z. Barnovska[5], A. Baroncelli[135a], G. Barone[49], A.J. Barr[120], F. Barreiro[82], J. Barreiro Guimarães da Costa[57], R. Bartoldus[144], A.E. Barton[72], P. Bartos[145a], V. Bartsch[150], A. Bassalat[117], A. Basye[166], R.L. Bates[53], S.J. Batista[159], J.R. Batley[28], M. Battaglia[138], M. Battistin[30], F. Bauer[137], H.S. Bawa[144,f], M.D. Beattie[72], T. Beau[80], P.H. Beauchemin[162], R. Beccherle[124a,124b], P. Bechtle[21], H.P. Beck[17], K. Becker[176], S. Becker[100], M. Beckingham[171], C. Becot[117], A.J. Beddall[19c], A. Beddall[19c], S. Bedikian[177], V.A. Bednyakov[65], C.P. Bee[149], L.J. Beemster[107], T.A. Beermann[176], M. Begel[25], K. Behr[120], C. Belanger-Champagne[87], P.J. Bell[49], W.H. Bell[49], G. Bella[154], L. Bellagamba[20a], A. Bellerive[29], M. Bellomo[86], K. Belotskiy[98], O. Beltramello[30], O. Benary[154], D. Benchekroun[136a], K. Bendtz[147a,147b], N. Benekos[166], Y. Benhammou[154], E. Benhar Noccioli[49], J.A. Benitez Garcia[160b], D.P. Benjamin[45], J.R. Bensinger[23], S. Bentvelsen[107], D. Berge[107], E. Bergeaas Kuutmann[167], N. Berger[5], F. Berghaus[170], J. Beringer[15], C. Bernard[22], P. Bernat[78], C. Bernius[79],

F.U. Bernlochner[170], T. Berry[77], P. Berta[129], C. Bertella[83], G. Bertoli[147a,147b], F. Bertolucci[124a,124b],
C. Bertsche[113], D. Bertsche[113], M.I. Besana[91a], G.J. Besjes[106], O. Bessidskaia[147a,147b], M. Bessner[42], N. Besson[137],
C. Betancourt[48], S. Bethke[101], W. Bhimji[46], R.M. Bianchi[125], L. Bianchini[23], M. Bianco[30], O. Biebel[100],
S.P. Bieniek[78], K. Bierwagen[54], J. Biesiada[15], M. Biglietti[135a], J. Bilbao De Mendizabal[49], H. Bilokon[47], M. Bindi[54],
S. Binet[117], A. Bingul[19c], C. Bini[133a,133b], C.W. Black[151], J.E. Black[144], K.M. Black[22], D. Blackburn[139],
R.E. Blair[6], J.-B. Blanchard[137], T. Blazek[145a], I. Bloch[42], C. Blocker[23], W. Blum[83,*], U. Blumenschein[54],
G.J. Bobbink[107], V.S. Bobrovnikov[109,c], S.S. Bocchetta[81], A. Bocci[45], C. Bock[100], C.R. Boddy[120], M. Boehler[48],
T.T. Boek[176], J.A. Bogaerts[30], A.G. Bogdanchikov[109], A. Bogouch[92,*], C. Bohm[147a], J. Bohm[127], V. Boisvert[77],
T. Bold[38a], V. Boldea[26a], A.S. Boldyrev[99], M. Bomben[80], M. Bona[76], M. Boonekamp[137], A. Borisov[130],
G. Borissov[72], M. Borri[84], S. Borroni[42], J. Bortfeldt[100], V. Bortolotto[60a], K. Bos[107], D. Boscherini[20a], M. Bosman[12],
H. Boterenbrood[107], J. Boudreau[125], J. Bouffard[2], E.V. Bouhova-Thacker[72], D. Boumediene[34], C. Bourdarios[117],
N. Bousson[114], S. Boutouil[136d], A. Boveia[31], J. Boyd[30], I.R. Boyko[65], I. Bozic[13a], J. Bracinik[18], A. Brandt[8],
G. Brandt[15], O. Brandt[58a], U. Bratzler[157], B. Brau[86], J.E. Brau[116], H.M. Braun[176,*], S.F. Brazzale[165a,165c],
B. Brelier[159], K. Brendlinger[122], A.J. Brennan[88], R. Brenner[167], S. Bressler[173], K. Bristow[146c], T.M. Bristow[46],
D. Britton[53], F.M. Brochu[28], I. Brock[21], R. Brock[90], J. Bronner[101], G. Brooijmans[35], T. Brooks[77], W.K. Brooks[32b],
J. Brosamer[15], E. Brost[116], J. Brown[55], P.A. Bruckman de Renstrom[39], D. Bruncko[145b], R. Bruneliere[48],
S. Brunet[61], A. Bruni[20a], G. Bruni[20a], M. Bruschi[20a], L. Bryngemark[81], T. Buanes[14], Q. Buat[143], F. Bucci[49],
P. Buchholz[142], A.G. Buckley[53], S.I. Buda[26a], I.A. Budagov[65], F. Buehrer[48], L. Bugge[119], M.K. Bugge[119],
O. Bulekov[98], A.C. Bundock[74], H. Burckhart[30], S. Burdin[74], B. Burghgrave[108], S. Burke[131], I. Burmeister[43],
E. Busato[34], D. Büscher[48], V. Büscher[83], P. Bussey[53], C.P. Buszello[167], B. Butler[57], J.M. Butler[22], A.I. Butt[3],
C.M. Buttar[53], J.M. Butterworth[78], P. Butti[107], W. Buttinger[28], A. Buzatu[53], M. Byszewski[10],
S. Cabrera Urbán[168], D. Caforio[20a,20b], O. Cakir[4a], P. Calafiura[15], A. Calandri[137], G. Calderini[80], P. Calfayan[100],
R. Calkins[108], L.P. Caloba[24a], D. Calvet[34], S. Calvet[34], R. Camacho Toro[49], S. Camarda[42], D. Cameron[119],
L.M. Caminada[15], R. Caminal Armadans[12], S. Campana[30], M. Campanelli[78], A. Campoverde[149], V. Canale[104a,104b],
A. Canepa[160a], M. Cano Bret[76], J. Cantero[82], R. Cantrill[126a], T. Cao[40], M.D.M. Capeans Garrido[30], I. Caprini[26a],
M. Caprini[26a], M. Capua[37a,37b], R. Caputo[83], R. Cardarelli[134a], T. Carli[30], G. Carlino[104a], L. Carminati[91a,91b],
S. Caron[106], E. Carquin[32a], G.D. Carrillo-Montoya[146c], J.R. Carter[28], J. Carvalho[126a,126c], D. Casadei[78],
M.P. Casado[12], M. Casolino[12], E. Castaneda-Miranda[146b], A. Castelli[107], V. Castillo Gimenez[168], N.F. Castro[126a],
P. Catastini[57], A. Catinaccio[30], J.R. Catmore[119], A. Cattai[30], G. Cattani[134a,134b], J. Caudron[83], V. Cavaliere[166],
D. Cavalli[91a], M. Cavalli-Sforza[12], V. Cavasinni[124a,124b], F. Ceradini[135a,135b], B.C. Cerio[45], K. Cerny[129],
A.S. Cerqueira[24b], A. Cerri[150], L. Cerrito[76], F. Cerutti[15], M. Cerv[30], A. Cervelli[17], S.A. Cetin[19b], A. Chafaq[136a],
D. Chakraborty[108], I. Chalupkova[129], P. Chang[166], B. Chapleau[87], J.D. Chapman[28], D. Charfeddine[117],
D.G. Charlton[18], C.C. Chau[159], C.A. Chavez Barajas[150], S. Cheatham[87], A. Chegwidden[90], S. Chekanov[6],
S.V. Chekulaev[160a], G.A. Chelkov[65,g], M.A. Chelstowska[89], C. Chen[64], H. Chen[25], K. Chen[149], L. Chen[33d,h],
S. Chen[33c], X. Chen[33f], Y. Chen[67], H.C. Cheng[89], Y. Cheng[31], A. Cheplakov[65], R. Cherkaoui El Moursli[136e],
V. Chernyatin[25,*], E. Cheu[7], L. Chevalier[137], V. Chiarella[47], G. Chiefari[104a,104b], J.T. Childers[6], A. Chilingarov[72],
G. Chiodini[73a], A.S. Chisholm[18], R.T. Chislett[78], A. Chitan[26a], M.V. Chizhov[65], S. Chouridou[9], B.K.B. Chow[100],
D. Chromek-Burckhart[30], M.L. Chu[152], J. Chudoba[127], J.J. Chwastowski[39], L. Chytka[115], G. Ciapetti[133a,133b],
A.K. Ciftci[4a], R. Ciftci[4a], D. Cinca[53], V. Cindro[75], A. Ciocio[15], Z.H. Citron[173], M. Citterio[91a], M. Ciubancan[26a],
A. Clark[49], P.J. Clark[46], R.N. Clarke[15], W. Cleland[125], J.C. Clemens[85], C. Clement[147a,147b], Y. Coadou[85],
M. Cobal[165a,165c], A. Coccaro[139], J. Cochran[64], L. Coffey[23], J.G. Cogan[144], B. Cole[35], S. Cole[108], A.P. Colijn[107],
J. Collot[55], T. Colombo[58c], G. Compostella[101], P. Conde Muiño[126a,126b], E. Coniavitis[48], S.H. Connell[146b],
I.A. Connelly[77], S.M. Consonni[91a,91b], V. Consorti[48], S. Constantinescu[26a], C. Conta[121a,121b], G. Conti[57],
F. Conventi[104a,i], M. Cooke[15], B.D. Cooper[78], A.M. Cooper-Sarkar[120], N.J. Cooper-Smith[77], K. Copic[15],
T. Cornelissen[176], M. Corradi[20a], F. Corriveau[87,j], A. Corso-Radu[164], A. Cortes-Gonzalez[12], G. Cortiana[101],
G. Costa[91a], M.J. Costa[168], D. Costanzo[140], D. Côté[8], G. Cottin[28], G. Cowan[77], B.E. Cox[84], K. Cranmer[110],
G. Cree[29], S. Crépé-Renaudin[55], F. Crescioli[80], W.A. Cribbs[147a,147b], M. Crispin Ortuzar[120], M. Cristinziani[21],
V. Croft[106], G. Crosetti[37a,37b], C.-M. Cuciuc[26a], T. Cuhadar Donszelmann[140], J. Cummings[177], M. Curatolo[47],
C. Cuthbert[151], H. Czirr[142], P. Czodrowski[3], S. D'Auria[53], M. D'Onofrio[74],
M.J. Da Cunha Sargedas De Sousa[126a,126b], C. Da Via[84], W. Dabrowski[38a], A. Dafinca[120], T. Dai[89], O. Dale[14],
F. Dallaire[95], C. Dallapiccola[86], M. Dam[36], A.C. Daniells[18], M. Dano Hoffmann[137], V. Dao[48], G. Darbo[50a],
S. Darmora[8], J.A. Dassoulas[42], A. Dattagupta[61], W. Davey[21], C. David[170], T. Davidek[129], E. Davies[120,d],
M. Davies[154], O. Davignon[80], A.R. Davison[78], P. Davison[78], Y. Davygora[58a], E. Dawe[143], I. Dawson[140],
R.K. Daya-Ishmukhametova[86], K. De[8], R. de Asmundis[104a], S. De Castro[20a,20b], S. De Cecco[80], N. De Groot[106],
P. de Jong[107], H. De la Torre[82], F. De Lorenzi[64], L. De Nooij[107], D. De Pedis[133a], A. De Salvo[133a], U. De Sanctis[150],
A. De Santo[150], J.B. De Vivie De Regie[117], W.J. Dearnaley[72], R. Debbe[25], C. Debenedetti[138], B. Dechenaux[55],
D.V. Dedovich[65], I. Deigaard[107], J. Del Peso[82], T. Del Prete[124a,124b], F. Deliot[137], C.M. Delitzsch[49],
M. Deliyergiyev[75], A. Dell'Acqua[30], L. Dell'Asta[22], M. Dell'Orso[124a,124b], M. Della Pietra[104a,i], D. della Volpe[49],

M. Delmastro[5], P.A. Delsart[55], C. Deluca[107], D.A. DeMarco[159], S. Demers[177], M. Demichev[65], A. Demilly[80],
S.P. Denisov[130], D. Derendarz[39], J.E. Derkaoui[136d], F. Derue[80], P. Dervan[74], K. Desch[21], C. Deterre[42],
P.O. Deviveiros[30], A. Dewhurst[131], S. Dhaliwal[107], A. Di Ciaccio[134a,134b], L. Di Ciaccio[5], A. Di Domenico[133a,133b],
C. Di Donato[104a,104b], A. Di Girolamo[30], B. Di Girolamo[30], A. Di Mattia[153], B. Di Micco[135a,135b], R. Di Nardo[47],
A. Di Simone[48], R. Di Sipio[20a,20b], D. Di Valentino[29], F.A. Dias[46], M.A. Diaz[32a], E.B. Diehl[89], J. Dietrich[16],
T.A. Dietzsch[58a], S. Diglio[85], A. Dimitrievska[13a], J. Dingfelder[21], P. Dita[26a], S. Dita[26a], F. Dittus[30], F. Djama[85],
T. Djobava[51b], J.I. Djuvsland[58a], M.A.B. do Vale[24c], D. Dobos[30], C. Doglioni[49], T. Doherty[53], T. Dohmae[156],
J. Dolejsi[129], Z. Dolezal[129], B.A. Dolgoshein[98,*], M. Donadelli[24d], S. Donati[124a,124b], P. Dondero[121a,121b],
J. Donini[34], J. Dopke[131], A. Doria[104a], M.T. Dova[71], A.T. Doyle[53], M. Dris[10], J. Dubbert[89], S. Dube[15],
E. Dubreuil[34], E. Duchovni[173], G. Duckeck[100], O.A. Ducu[26a], D. Duda[176], A. Dudarev[30], F. Dudziak[64], L. Duflot[117],
L. Duguid[77], M. Dührssen[30], M. Dunford[58a], H. Duran Yildiz[4a], M. Düren[52], A. Durglishvili[51b], M. Dwuznik[38a],
M. Dyndal[38a], J. Ebke[100], W. Edson[2], N.C. Edwards[46], W. Ehrenfeld[21], T. Eifert[144], G. Eigen[14], K. Einsweiler[15],
T. Ekelof[167], M. El Kacimi[136c], M. Ellert[167], S. Elles[5], F. Ellinghaus[83], N. Ellis[30], J. Elmsheuser[100], M. Elsing[30],
D. Emeliyanov[131], Y. Enari[156], O.C. Endner[83], M. Endo[118], R. Engelmann[149], J. Erdmann[177], A. Ereditato[17],
D. Eriksson[147a], G. Ernis[176], J. Ernst[2], M. Ernst[25], J. Ernwein[137], D. Errede[166], S. Errede[166], E. Ertel[83],
M. Escalier[117], H. Esch[43], C. Escobar[125], B. Esposito[47], A.I. Etienvre[137], E. Etzion[154], H. Evans[61], A. Ezhilov[123],
L. Fabbri[20a,20b], G. Facini[31], R.M. Fakhrutdinov[130], S. Falciano[133a], R.J. Falla[78], J. Faltova[129], Y. Fang[33a],
M. Fanti[91a,91b], A. Farbin[8], A. Farilla[135a], T. Farooque[12], S. Farrell[15], S.M. Farrington[171], P. Farthouat[30],
F. Fassi[136e], P. Fassnacht[30], D. Fassouliotis[9], A. Favareto[50a,50b], L. Fayard[117], P. Federic[145a], O.L. Fedin[123,k],
W. Fedorko[169], M. Fehling-Kaschek[48], S. Feigl[30], L. Feligioni[85], C. Feng[33d], E.J. Feng[6], H. Feng[89], A.B. Fenyuk[130],
S. Fernandez Perez[30], S. Ferrag[53], J. Ferrando[53], A. Ferrari[167], P. Ferrari[107], R. Ferrari[121a], D.E. Ferreira de Lima[53],
A. Ferrer[168], D. Ferrere[49], C. Ferretti[89], A. Ferretto Parodi[50a,50b], M. Fiascaris[31], F. Fiedler[83], A. Filipčič[75],
M. Filipuzzi[42], F. Filthaut[106], M. Fincke-Keeler[170], K.D. Finelli[151], M.C.N. Fiolhais[126a,126c], L. Fiorini[168],
A. Firan[40], A. Fischer[2], J. Fischer[176], W.C. Fisher[90], E.A. Fitzgerald[23], M. Flechl[48], I. Fleck[142], P. Fleischmann[89],
S. Fleischmann[176], G.T. Fletcher[140], G. Fletcher[76], T. Flick[176], A. Floderus[81], L.R. Flores Castillo[60a],
M.J. Flowerdew[101], A. Formica[137], A. Forti[84], D. Fortin[160a], D. Fournier[117], H. Fox[72], S. Fracchia[12],
P. Francavilla[80], M. Franchini[20a,20b], S. Franchino[30], D. Francis[30], L. Franconi[119], M. Franklin[57], S. Franz[62],
M. Fraternali[121a,121b], S.T. French[28], C. Friedrich[42], F. Friedrich[44], D. Froidevaux[30], J.A. Frost[28], C. Fukunaga[157],
E. Fullana Torregrosa[83], B.G. Fulsom[144], J. Fuster[168], C. Gabaldon[55], O. Gabizon[176], A. Gabrielli[20a,20b],
A. Gabrielli[133a,133b], S. Gadatsch[107], S. Gadomski[49], G. Gagliardi[50a,50b], P. Gagnon[61], C. Galea[106],
B. Galhardo[126a,126c], E.J. Gallas[120], V. Gallo[17], B.J. Gallop[131], P. Gallus[128], G. Galster[36], K.K. Gan[111],
J. Gao[33b,h], Y.S. Gao[144,f], F.M. Garay Walls[46], F. Garberson[177], C. García[168], J.E. García Navarro[168],
M. Garcia-Sciveres[15], R.W. Gardner[31], N. Garelli[144], V. Garonne[30], C. Gatti[47], G. Gaudio[121a], B. Gaur[142],
L. Gauthier[95], P. Gauzzi[133a,133b], I.L. Gavrilenko[96], C. Gay[169], G. Gaycken[21], E.N. Gazis[10], P. Ge[33d], Z. Gecse[169],
C.N.P. Gee[131], D.A.A. Geerts[107], Ch. Geich-Gimbel[21], K. Gellerstedt[147a,147b], C. Gemme[50a], A. Gemmell[53],
M.H. Genest[55], S. Gentile[133a,133b], M. George[54], S. George[77], D. Gerbaudo[164], A. Gershon[154], H. Ghazlane[136b],
N. Ghodbane[34], B. Giacobbe[20a], S. Giagu[133a,133b], V. Giangiobbe[12], P. Giannetti[124a,124b], F. Gianotti[30],
B. Gibbard[25], S.M. Gibson[77], M. Gilchriese[15], T.P.S. Gillam[28], D. Gillberg[30], G. Gilles[34], D.M. Gingrich[3,e],
N. Giokaris[9], M.P. Giordani[165a,165c], R. Giordano[104a,104b], F.M. Giorgi[20a], F.M. Giorgi[16], P.F. Giraud[137],
D. Giugni[91a], C. Giuliani[48], M. Giulini[58b], B.K. Gjelsten[119], S. Gkaitatzis[155], I. Gkialas[155,l], E.L. Gkougkousis[117],
L.K. Gladilin[99], C. Glasman[82], J. Glatzer[30], P.C.F. Glaysher[46], A. Glazov[42], G.L. Glonti[65], M. Goblirsch-Kolb[101],
J.R. Goddard[76], J. Godlewski[30], C. Goeringer[83], S. Goldfarb[89], T. Golling[177], D. Golubkov[130],
A. Gomes[126a,126b,126d], L.S. Gomez Fajardo[42], R. Gonçalo[126a], J. Goncalves Pinto Firmino Da Costa[137],
L. Gonella[21], S. González de la Hoz[168], G. Gonzalez Parra[12], S. Gonzalez-Sevilla[49], L. Goossens[30],
P.A. Gorbounov[97], H.A. Gordon[25], I. Gorelov[105], B. Gorini[30], E. Gorini[73a,73b], A. Gorišek[75], E. Gornicki[39],
A.T. Goshaw[45], C. Gössling[43], M.I. Gostkin[65], M. Gouighri[136a], D. Goujdami[136c], M.P. Goulette[49],
A.G. Goussiou[139], C. Goy[5], H.M.X. Grabas[138], L. Graber[54], I. Grabowska-Bold[38a], P. Grafström[20a,20b],
K-J. Grahn[42], J. Gramling[49], E. Gramstad[119], S. Grancagnolo[16], V. Grassi[149], V. Gratchev[123], H.M. Gray[30],
E. Graziani[135a], O.G. Grebenyuk[123], Z.D. Greenwood[79,m], K. Gregersen[78], I.M. Gregor[42], P. Grenier[144],
J. Griffiths[8], A.A. Grillo[138], K. Grimm[72], S. Grinstein[12,n], Ph. Gris[34], Y.V. Grishkevich[99], J.-F. Grivaz[117],
J.P. Grohs[44], A. Grohsjean[42], E. Gross[173], J. Grosse-Knetter[54], G.C. Grossi[134a,134b], J. Groth-Jensen[173],
Z.J. Grout[150], L. Guan[33b], J. Guenther[128], F. Guescini[49], D. Guest[177], O. Gueta[154], C. Guicheney[34],
E. Guido[50a,50b], T. Guillemin[117], S. Guindon[2], U. Gul[53], C. Gumpert[44], J. Guo[35], S. Gupta[120], P. Gutierrez[113],
N.G. Gutierrez Ortiz[53], C. Gutschow[78], N. Guttman[154], C. Guyot[137], C. Gwenlan[120], C.B. Gwilliam[74], A. Haas[110],
C. Haber[15], H.K. Hadavand[8], N. Haddad[136e], P. Haefner[21], S. Hageböck[21], Z. Hajduk[39], H. Hakobyan[178],
M. Haleem[42], D. Hall[120], G. Halladjian[90], G.D. Hallewell[85], K. Hamacher[176], P. Hamal[115], K. Hamano[170],
M. Hamer[54], A. Hamilton[146a], S. Hamilton[162], G.N. Hamity[146c], P.G. Hamnett[42], L. Han[33b], K. Hanagaki[118],
K. Hanawa[156], M. Hance[15], P. Hanke[58a], R. Hanna[137], J.B. Hansen[36], J.D. Hansen[36], P.H. Hansen[36], K. Hara[161],

A.S. Hard[174], T. Harenberg[176], F. Hariri[117], S. Harkusha[92], D. Harper[89], R.D. Harrington[46], O.M. Harris[139],
P.F. Harrison[171], F. Hartjes[107], M. Hasegawa[67], S. Hasegawa[103], Y. Hasegawa[141], A. Hasib[113], S. Hassani[137],
S. Haug[17], M. Hauschild[30], R. Hauser[90], M. Havranek[127], C.M. Hawkes[18], R.J. Hawkings[30], A.D. Hawkins[81],
T. Hayashi[161], D. Hayden[90], C.P. Hays[120], H.S. Hayward[74], S.J. Haywood[131], S.J. Head[18], T. Heck[83], V. Hedberg[81],
L. Heelan[8], S. Heim[122], T. Heim[176], B. Heinemann[15], L. Heinrich[110], J. Hejbal[127], L. Helary[22], C. Heller[100],
M. Heller[30], S. Hellman[147a,147b], D. Hellmich[21], C. Helsens[30], J. Henderson[120], R.C.W. Henderson[72], Y. Heng[174],
C. Hengler[42], A. Henrichs[177], A.M. Henriques Correia[30], S. Henrot-Versille[117], G.H. Herbert[16],
Y. Hernández Jiménez[168], R. Herrberg-Schubert[16], G. Herten[48], R. Hertenberger[100], L. Hervas[30], G.G. Hesketh[78],
N.P. Hessey[107], R. Hickling[76], E. Higón-Rodriguez[168], E. Hill[170], J.C. Hill[28], K.H. Hiller[42], S. Hillert[21], S.J. Hillier[18],
I. Hinchliffe[15], E. Hines[122], M. Hirose[158], D. Hirschbuehl[176], J. Hobbs[149], N. Hod[107], M.C. Hodgkinson[140],
P. Hodgson[140], A. Hoecker[30], M.R. Hoeferkamp[105], F. Hoenig[100], J. Hoffman[40], D. Hoffmann[85], M. Hohlfeld[83],
T.R. Holmes[15], T.M. Hong[122], L. Hooft van Huysduynen[110], W.H. Hopkins[116], Y. Horii[103], J-Y. Hostachy[55],
S. Hou[152], A. Hoummada[136a], J. Howard[120], J. Howarth[42], M. Hrabovsky[115], I. Hristova[16], J. Hrivnac[117],
T. Hryn'ova[5], C. Hsu[146c], P.J. Hsu[83], S.-C. Hsu[139], D. Hu[35], X. Hu[89], Y. Huang[42], Z. Hubacek[30], F. Hubaut[85],
F. Huegging[21], T.B. Huffman[120], E.W. Hughes[35], G. Hughes[72], M. Huhtinen[30], T.A. Hülsing[83], M. Hurwitz[15],
N. Huseynov[65,b], J. Huston[90], J. Huth[57], G. Iacobucci[49], G. Iakovidis[10], I. Ibragimov[142], L. Iconomidou-Fayard[117],
E. Ideal[177], Z. Idrissi[136e], P. Iengo[104a], O. Igonkina[107], T. Iizawa[172], Y. Ikegami[66], K. Ikematsu[142], M. Ikeno[66],
Y. Ilchenko[31,o], D. Iliadis[155], N. Ilic[159], Y. Inamaru[67], T. Ince[101], P. Ioannou[9], M. Iodice[135a], K. Iordanidou[9],
V. Ippolito[57], A. Irles Quiles[168], C. Isaksson[167], M. Ishino[68], M. Ishitsuka[158], R. Ishmukhametov[111], C. Issever[120],
S. Istin[19a], J.M. Iturbe Ponce[84], R. Iuppa[134a,134b], J. Ivarsson[81], W. Iwanski[39], H. Iwasaki[66], J.M. Izen[41],
V. Izzo[104a], B. Jackson[122], M. Jackson[74], P. Jackson[1], M.R. Jaekel[30], V. Jain[2], K. Jakobs[48], S. Jakobsen[30],
T. Jakoubek[127], J. Jakubek[128], D.O. Jamin[152], D.K. Jana[79], E. Jansen[78], H. Jansen[30], J. Janssen[21], M. Janus[171],
G. Jarlskog[81], N. Javadov[65,b], T. Javůrek[48], L. Jeanty[15], J. Jejelava[51a,p], G.-Y. Jeng[151], D. Jennens[88], P. Jenni[48,q],
J. Jentzsch[43], C. Jeske[171], S. Jézéquel[5], H. Ji[174], J. Jia[149], Y. Jiang[33b], M. Jimenez Belenguer[42], S. Jin[33a],
A. Jinaru[26a], O. Jinnouchi[158], M.D. Joergensen[36], K.E. Johansson[147a,147b], P. Johansson[140], K.A. Johns[7],
K. Jon-And[147a,147b], G. Jones[171], R.W.L. Jones[72], T.J. Jones[74], J. Jongmanns[58a], P.M. Jorge[126a,126b], K.D. Joshi[84],
J. Jovicevic[148], X. Ju[174], C.A. Jung[43], R.M. Jungst[30], P. Jussel[62], A. Juste Rozas[12,n], M. Kaci[168], A. Kaczmarska[39],
M. Kado[117], H. Kagan[111], M. Kagan[144], E. Kajomovitz[45], C.W. Kalderon[120], S. Kama[40], A. Kamenshchikov[130],
N. Kanaya[156], M. Kaneda[30], S. Kaneti[28], V.A. Kantserov[98], J. Kanzaki[66], B. Kaplan[110], A. Kapliy[31], D. Kar[53],
K. Karakostas[10], N. Karastathis[10], M.J. Kareem[54], M. Karnevskiy[83], S.N. Karpov[65], Z.M. Karpova[65],
K. Karthik[110], V. Kartvelishvili[72], A.N. Karyukhin[130], L. Kashif[174], G. Kasieczka[58b], R.D. Kass[111], A. Kastanas[14],
Y. Kataoka[156], A. Katre[49], J. Katzy[42], V. Kaushik[7], K. Kawagoe[70], T. Kawamoto[156], G. Kawamura[54],
S. Kazama[156], V.F. Kazanin[109], M.Y. Kazarinov[65], R. Keeler[170], R. Kehoe[40], M. Keil[54], J.S. Keller[42],
J.J. Kempster[77], H. Keoshkerian[5], O. Kepka[127], B.P. Kerševan[75], S. Kersten[176], K. Kessoku[156], J. Keung[159],
R.A. Keyes[87], F. Khalil-zada[11], H. Khandanyan[147a,147b], A. Khanov[114], A. Kharlamov[109], A. Khodinov[98],
A. Khomich[58a], T.J. Khoo[28], G. Khoriauli[21], A. Khoroshilov[176], V. Khovanskiy[97], E. Khramov[65], J. Khubua[51b],
H.Y. Kim[8], H. Kim[147a,147b], S.H. Kim[161], N. Kimura[172], O. Kind[16], B.T. King[74], M. King[168], R.S.B. King[120],
S.B. King[169], J. Kirk[131], A.E. Kiryunin[101], T. Kishimoto[67], D. Kisielewska[38a], F. Kiss[48], K. Kiuchi[161],
E. Kladiva[145b], M. Klein[74], U. Klein[74], K. Kleinknecht[83], P. Klimek[147a,147b], A. Klimentov[25], R. Klingenberg[43],
J.A. Klinger[84], T. Klioutchnikova[30], P.F. Klok[106], E.-E. Kluge[58a], P. Kluit[107], S. Kluth[101], E. Kneringer[62],
E.B.F.G. Knoops[85], A. Knue[53], D. Kobayashi[158], T. Kobayashi[156], M. Kobel[44], M. Kocian[144], P. Kodys[129],
T. Koffas[29], E. Koffeman[107], L.A. Kogan[120], S. Kohlmann[176], Z. Kohout[128], T. Kohriki[66], T. Koi[144],
H. Kolanoski[16], I. Koletsou[5], J. Koll[90], A.A. Komar[96,*], Y. Komori[156], T. Kondo[66], N. Kondrashova[42],
K. Köneke[48], A.C. König[106], S. König[83], T. Kono[66,r], R. Konoplich[110,s], N. Konstantinidis[78], R. Kopeliansky[153],
S. Koperny[38a], L. Köpke[83], A.K. Kopp[48], K. Korcyl[39], K. Kordas[155], A. Korn[78], A.A. Korol[109,c], I. Korolkov[12],
E.V. Korolkova[140], V.A. Korotkov[130], O. Kortner[101], S. Kortner[101], V.V. Kostyukhin[21], V.M. Kotov[65], A. Kotwal[45],
A. Kourkoumeli-Charalampidi[155], C. Kourkoumelis[9], V. Kouskoura[155], A. Koutsman[160a], R. Kowalewski[170],
T.Z. Kowalski[38a], W. Kozanecki[137], A.S. Kozhin[130], V.A. Kramarenko[99], G. Kramberger[75], D. Krasnopevtsev[98],
M.W. Krasny[80], A. Krasznahorkay[30], J.K. Kraus[21], A. Kravchenko[25], S. Kreiss[110], M. Kretz[58c], J. Kretzschmar[74],
K. Kreutzfeldt[52], P. Krieger[159], K. Kroeninger[54], H. Kroha[101], J. Kroll[122], J. Kroseberg[21], J. Krstic[13a],
U. Kruchonak[65], H. Krüger[21], T. Kruker[17], N. Krumnack[64], Z.V. Krumshteyn[65], A. Kruse[174], M.C. Kruse[45],
M. Kruskal[22], T. Kubota[88], H. Kucuk[78], S. Kuday[4c], S. Kuehn[48], A. Kugel[58c], A. Kuhl[138], T. Kuhl[42], V. Kukhtin[65],
Y. Kulchitsky[92], S. Kuleshov[32b], M. Kuna[133a,133b], T. Kunigo[68], A. Kupco[127], H. Kurashige[67], Y.A. Kurochkin[92],
R. Kurumida[67], V. Kus[127], E.S. Kuwertz[148], M. Kuze[158], J. Kvita[115], A. La Rosa[49], L. La Rotonda[37a,37b],
C. Lacasta[168], F. Lacava[133a,133b], J. Lacey[29], H. Lacker[16], D. Lacour[80], V.R. Lacuesta[168], E. Ladygin[65], R. Lafaye[5],
B. Laforge[80], T. Lagouri[177], S. Lai[48], H. Laier[58a], L. Lambourne[78], S. Lammers[61], C.L. Lampen[7], W. Lampl[7],
E. Lançon[137], U. Landgraf[48], M.P.J. Landon[76], V.S. Lang[58a], A.J. Lankford[164], F. Lanni[25], K. Lantzsch[30],
S. Laplace[80], C. Lapoire[21], J.F. Laporte[137], T. Lari[91a], F. Lasagni Manghi[20a,20b], M. Lassnig[30], P. Laurelli[47],

W. Lavrijsen[15], A.T. Law[138], P. Laycock[74], O. Le Dortz[80], E. Le Guirriec[85], E. Le Menedeu[12], T. LeCompte[6],
F. Ledroit-Guillon[55], C.A. Lee[146b], H. Lee[107], J.S.H. Lee[118], S.C. Lee[152], L. Lee[1], G. Lefebvre[80], M. Lefebvre[170],
F. Legger[100], C. Leggett[15], A. Lehan[74], G. Lehmann Miotto[30], X. Lei[7], W.A. Leight[29], A. Leisos[155], A.G. Leister[177],
M.A.L. Leite[24d], R. Leitner[129], D. Lellouch[173], B. Lemmer[54], K.J.C. Leney[78], T. Lenz[21], G. Lenzen[176], B. Lenzi[30],
R. Leone[7], S. Leone[124a,124b], C. Leonidopoulos[46], S. Leontsinis[10], C. Leroy[95], C.G. Lester[28], C.M. Lester[122],
M. Levchenko[123], J. Levêque[5], D. Levin[89], L.J. Levinson[173], M. Levy[18], A. Lewis[120], G.H. Lewis[110], A.M. Leyko[21],
M. Leyton[41], B. Li[33b,t], B. Li[85], H. Li[149], H.L. Li[31], L. Li[45], L. Li[33e], S. Li[45], Y. Li[33c,u], Z. Liang[138], H. Liao[34],
B. Liberti[134a], P. Lichard[30], K. Lie[166], J. Liebal[21], W. Liebig[14], C. Limbach[21], A. Limosani[151], S.C. Lin[152,v],
T.H. Lin[83], F. Linde[107], B.E. Lindquist[149], J.T. Linnemann[90], E. Lipeles[122], A. Lipniacka[14], M. Lisovyi[42],
T.M. Liss[166], D. Lissauer[25], A. Lister[169], A.M. Litke[138], B. Liu[152], D. Liu[152], J.B. Liu[33b], K. Liu[33b,w], L. Liu[89],
M. Liu[45], M. Liu[33b], Y. Liu[33b], M. Livan[121a,121b], A. Lleres[55], J. Llorente Merino[82], S.L. Lloyd[76], F. Lo Sterzo[152],
E. Lobodzinska[42], P. Loch[7], W.S. Lockman[138], T. Loddenkoetter[21], F.K. Loebinger[84], A.E. Loevschall-Jensen[36],
A. Loginov[177], T. Lohse[16], K. Lohwasser[42], M. Lokajicek[127], V.P. Lombardo[5], B.A. Long[22], J.D. Long[89],
R.E. Long[72], L. Lopes[126a], D. Lopez Mateos[57], B. Lopez Paredes[140], I. Lopez Paz[12], J. Lorenz[100],
N. Lorenzo Martinez[61], M. Losada[163], P. Loscutoff[15], X. Lou[41], A. Lounis[117], J. Love[6], P.A. Love[72], A.J. Lowe[144,f],
F. Lu[33a], N. Lu[89], H.J. Lubatti[139], C. Luci[133a,133b], A. Lucotte[55], F. Luehring[61], W. Lukas[62], L. Luminari[133a],
O. Lundberg[147a,147b], B. Lund-Jensen[148], M. Lungwitz[83], D. Lynn[25], R. Lysak[127], E. Lytken[81], H. Ma[25],
L.L. Ma[33d], G. Maccarrone[47], A. Macchiolo[101], J. Machado Miguens[126a,126b], D. Macina[30], D. Madaffari[85],
R. Madar[48], H.J. Maddocks[72], W.F. Mader[44], A. Madsen[167], M. Maeno[8], T. Maeno[25], A. Maevskiy[99],
E. Magradze[54], K. Mahboubi[48], J. Mahlstedt[107], S. Mahmoud[74], C. Maiani[137], C. Maidantchik[24a], A.A. Maier[101],
A. Maio[126a,126b,126d], S. Majewski[116], Y. Makida[66], N. Makovec[117], P. Mal[137,x], B. Malaescu[80], Pa. Malecki[39],
V.P. Maleev[123], F. Malek[55], U. Mallik[63], D. Malon[6], C. Malone[144], S. Maltezos[10], V.M. Malyshev[109],
S. Malyukov[30], J. Mamuzic[13b], B. Mandelli[30], L. Mandelli[91a], I. Mandić[75], R. Mandrysch[63], J. Maneira[126a,126b],
A. Manfredini[101], L. Manhaes de Andrade Filho[24b], J.A. Manjarres Ramos[160b], A. Mann[100], P.M. Manning[138],
A. Manousakis-Katsikakis[9], B. Mansoulie[137], R. Mantifel[87], L. Mapelli[30], L. March[146c], J.F. Marchand[29],
G. Marchiori[80], M. Marcisovsky[127], C.P. Marino[170], M. Marjanovic[13a], F. Marroquim[24a], S.P. Marsden[84],
Z. Marshall[15], L.F. Marti[17], S. Marti-Garcia[168], B. Martin[30], B. Martin[90], T.A. Martin[171], V.J. Martin[46],
B. Martin dit Latour[14], H. Martinez[137], M. Martinez[12,n], S. Martin-Haugh[131], A.C. Martyniuk[78], M. Marx[139],
F. Marzano[133a], A. Marzin[30], L. Masetti[83], T. Mashimo[156], R. Mashinistov[96], J. Masik[84], A.L. Maslennikov[109,c],
I. Massa[20a,20b], L. Massa[20a,20b], N. Massol[5], P. Mastrandrea[149], A. Mastroberardino[37a,37b], T. Masubuchi[156],
P. Mättig[176], J. Mattmann[83], J. Maurer[26a], S.J. Maxfield[74], D.A. Maximov[109,c], R. Mazini[152],
L. Mazzaferro[134a,134b], G. Mc Goldrick[159], S.P. Mc Kee[89], A. McCarn[89], R.L. McCarthy[149], T.G. McCarthy[29],
N.A. McCubbin[131], K.W. McFarlane[56,*], J.A. Mcfayden[78], G. Mchedlidze[54], S.J. McMahon[131],
R.A. McPherson[170,j], J. Mechnich[107], M. Medinnis[42], S. Meehan[31], S. Mehlhase[100], A. Mehta[74], K. Meier[58a],
C. Meineck[100], B. Meirose[81], C. Melachrinos[31], B.R. Mellado Garcia[146c], F. Meloni[17], A. Mengarelli[20a,20b],
S. Menke[101], E. Meoni[162], K.M. Mercurio[57], S. Mergelmeyer[21], N. Meric[137], P. Mermod[49], L. Merola[104a,104b],
C. Meroni[91a], F.S. Merritt[31], H. Merritt[111], A. Messina[30,y], J. Metcalfe[25], A.S. Mete[164], C. Meyer[83], C. Meyer[122],
J-P. Meyer[137], J. Meyer[30], R.P. Middleton[131], S. Migas[74], L. Mijović[21], G. Mikenberg[173], M. Mikestikova[127],
M. Mikuž[75], A. Milic[30], D.W. Miller[31], C. Mills[46], A. Milov[173], D.A. Milstead[147a,147b], A.A. Minaenko[130],
Y. Minami[156], I.A. Minashvili[65], A.I. Mincer[110], B. Mindur[38a], M. Mineev[65], Y. Ming[174], L.M. Mir[12],
G. Mirabelli[133a], T. Mitani[172], J. Mitrevski[100], V.A. Mitsou[168], A. Miucci[49], P.S. Miyagawa[140], J.U. Mjörnmark[81],
T. Moa[147a,147b], K. Mochizuki[85], S. Mohapatra[35], W. Mohr[48], S. Molander[147a,147b], R. Moles-Valls[168], K. Mönig[42],
C. Monini[55], J. Monk[36], E. Monnier[85], J. Montejo Berlingen[12], F. Monticelli[71], S. Monzani[133a,133b], R.W. Moore[3],
N. Morange[63], D. Moreno[83], M. Moreno Llácer[54], P. Morettini[50a], M. Morgenstern[44], M. Morii[57], V. Morisbak[119],
S. Moritz[83], A.K. Morley[148], G. Mornacchi[30], J.D. Morris[76], L. Morvaj[103], H.G. Moser[101], M. Mosidze[51b],
J. Moss[111], K. Motohashi[158], R. Mount[144], E. Mountricha[25], S.V. Mouraviev[96,*], E.J.W. Moyse[86], S. Muanza[85],
R.D. Mudd[18], F. Mueller[58a], J. Mueller[125], K. Mueller[21], T. Mueller[28], T. Mueller[83], D. Muenstermann[49],
Y. Munwes[154], J.A. Murillo Quijada[18], W.J. Murray[171,131], H. Musheghyan[54], E. Musto[153], A.G. Myagkov[130,z],
M. Myska[128], O. Nackenhorst[54], J. Nadal[54], K. Nagai[120], R. Nagai[158], Y. Nagai[85], K. Nagano[66], A. Nagarkar[111],
Y. Nagasaka[59], K. Nagata[161], M. Nagel[101], A.M. Nairz[30], Y. Nakahama[30], K. Nakamura[66], T. Nakamura[156],
I. Nakano[112], H. Namasivayam[41], G. Nanava[21], R.F. Naranjo Garcia[42], R. Narayan[58b], T. Nattermann[21],
T. Naumann[42], G. Navarro[163], R. Nayyar[7], H.A. Neal[89], P.Yu. Nechaeva[96], T.J. Neep[84], P.D. Nef[144],
A. Negri[121a,121b], G. Negri[30], M. Negrini[20a], S. Nektarijevic[49], C. Nellist[117], A. Nelson[164], T.K. Nelson[144],
S. Nemecek[127], P. Nemethy[110], A.A. Nepomuceno[24a], M. Nessi[30,aa], M.S. Neubauer[166], M. Neumann[176],
R.M. Neves[110], P. Nevski[25], P.R. Newman[18], D.H. Nguyen[6], R.B. Nickerson[120], R. Nicolaidou[137], B. Nicquevert[30],
J. Nielsen[138], N. Nikiforou[35], A. Nikiforov[16], V. Nikolaenko[130,z], I. Nikolic-Audit[80], K. Nikolics[49],
K. Nikolopoulos[18], P. Nilsson[25], Y. Ninomiya[156], A. Nisati[133a], R. Nisius[101], T. Nobe[158], L. Nodulman[6],
M. Nomachi[118], I. Nomidis[29], S. Norberg[113], M. Nordberg[30], O. Novgorodova[44], S. Nowak[101], M. Nozaki[66],

L. Nozka[115], K. Ntekas[10], G. Nunes Hanninger[88], T. Nunnemann[100], E. Nurse[78], F. Nuti[88], B.J. O'Brien[46],
F. O'grady[7], D.C. O'Neil[143], V. O'Shea[53], F.G. Oakham[29,e], H. Oberlack[101], T. Obermann[21], J. Ocariz[80],
A. Ochi[67], M.I. Ochoa[78], S. Oda[70], S. Odaka[66], H. Ogren[61], A. Oh[84], S.H. Oh[45], C.C. Ohm[15], H. Ohman[167],
H. Oide[30], W. Okamura[118], H. Okawa[25], Y. Okumura[31], T. Okuyama[156], A. Olariu[26a], A.G. Olchevski[65],
S.A. Olivares Pino[46], D. Oliveira Damazio[25], E. Oliver Garcia[168], A. Olszewski[39], J. Olszowska[39], A. Onofre[126a,126e],
P.U.E. Onyisi[31,o], C.J. Oram[160a], M.J. Oreglia[31], Y. Oren[154], D. Orestano[135a,135b], N. Orlando[73a,73b],
C. Oropeza Barrera[53], R.S. Orr[159], B. Osculati[50a,50b], R. Ospanov[122], G. Otero y Garzon[27], H. Otono[70],
M. Ouchrif[136d], E.A. Ouellette[170], F. Ould-Saada[119], A. Ouraou[137], K.P. Oussoren[107], Q. Ouyang[33a],
A. Ovcharova[15], M. Owen[84], V.E. Ozcan[19a], N. Ozturk[8], K. Pachal[120], A. Pacheco Pages[12], C. Padilla Aranda[12],
M. Pagáčová[48], S. Pagan Griso[15], E. Paganis[140], C. Pahl[101], F. Paige[25], P. Pais[86], K. Pajchel[119], G. Palacino[160b],
S. Palestini[30], M. Palka[38b], D. Pallin[34], A. Palma[126a,126b], J.D. Palmer[18], Y.B. Pan[174], E. Panagiotopoulou[10],
J.G. Panduro Vazquez[77], P. Pani[107], N. Panikashvili[89], S. Panitkin[25], D. Pantea[26a], L. Paolozzi[134a,134b],
Th.D. Papadopoulou[10], K. Papageorgiou[155,l], A. Paramonov[6], D. Paredes Hernandez[155], M.A. Parker[28],
F. Parodi[50a,50b], J.A. Parsons[35], U. Parzefall[48], E. Pasqualucci[133a], S. Passaggio[50a], A. Passeri[135a],
F. Pastore[135a,135b,∗], Fr. Pastore[77], G. Pásztor[29], S. Pataraia[176], N.D. Patel[151], J.R. Pater[84], S. Patricelli[104a,104b],
T. Pauly[30], J. Pearce[170], L.E. Pedersen[36], M. Pedersen[119], S. Pedraza Lopez[168], R. Pedro[126a,126b],
S.V. Peleganchuk[109], D. Pelikan[167], H. Peng[33b], B. Penning[31], J. Penwell[61], D.V. Perepelitsa[25], E. Perez Codina[160a],
M.T. Pérez García-Estañ[168], L. Perini[91a,91b], H. Pernegger[30], S. Perrella[104a,104b], R. Perrino[73a], R. Peschke[42],
V.D. Peshekhonov[65], K. Peters[30], R.F.Y. Peters[84], B.A. Petersen[30], T.C. Petersen[36], E. Petit[42], A. Petridis[147a,147b],
C. Petridou[155], E. Petrolo[133a], F. Petrucci[135a,135b], N.E. Pettersson[158], R. Pezoa[32b], P.W. Phillips[131],
G. Piacquadio[144], E. Pianori[171], A. Picazio[49], E. Piccaro[76], M. Piccinini[20a,20b], R. Piegaia[27], D.T. Pignotti[111],
J.E. Pilcher[31], A.D. Pilkington[78], J. Pina[126a,126b,126d], M. Pinamonti[165a,165c,ab], A. Pinder[120], J.L. Pinfold[3],
A. Pingel[36], B. Pinto[126a], S. Pires[80], M. Pitt[173], C. Pizio[91a,91b], L. Plazak[145a], M.-A. Pleier[25], V. Pleskot[129],
E. Plotnikova[65], P. Plucinski[147a,147b], D. Pluth[64], S. Poddar[58a], F. Podlyski[34], R. Poettgen[83], L. Poggioli[117],
D. Pohl[21], M. Pohl[49], G. Polesello[121a], A. Policicchio[37a,37b], R. Polifka[159], A. Polini[20a], C.S. Pollard[45],
V. Polychronakos[25], K. Pommès[30], L. Pontecorvo[133a], B.G. Pope[90], G.A. Popeneciu[26b], D.S. Popovic[13a],
A. Poppleton[30], X. Portell Bueso[12], S. Pospisil[128], K. Potamianos[15], I.N. Potrap[65], C.J. Potter[150], C.T. Potter[116],
G. Poulard[30], J. Poveda[61], V. Pozdnyakov[65], P. Pralavorio[85], A. Pranko[15], S. Prasad[30], R. Pravahan[8], S. Prell[64],
D. Price[84], J. Price[74], L.E. Price[6], D. Prieur[125], M. Primavera[73a], M. Proissl[46], K. Prokofiev[47], F. Prokoshin[32b],
E. Protopapadaki[137], S. Protopopescu[25], J. Proudfoot[6], M. Przybycien[38a], H. Przysiezniak[5], E. Ptacek[116],
D. Puddu[135a,135b], E. Pueschel[86], D. Puldon[149], M. Purohit[25,ac], P. Puzo[117], J. Qian[89], G. Qin[53], Y. Qin[84],
A. Quadt[54], D.R. Quarrie[15], W.B. Quayle[165a,165b], M. Queitsch-Maitland[84], D. Quilty[53], A. Qureshi[160b],
V. Radeka[25], V. Radescu[42], S.K. Radhakrishnan[149], P. Radloff[116], P. Rados[88], F. Ragusa[91a,91b], G. Rahal[179],
S. Rajagopalan[25], M. Rammensee[30], A.S. Randle-Conde[40], C. Rangel-Smith[167], K. Rao[164], F. Rauscher[100],
T.C. Rave[48], T. Ravenscroft[53], M. Raymond[30], A.L. Read[119], N.P. Readioff[74], D.M. Rebuzzi[121a,121b],
A. Redelbach[175], G. Redlinger[25], R. Reece[138], K. Reeves[41], L. Rehnisch[16], H. Reisin[27], M. Relich[164], C. Rembser[30],
H. Ren[33a], Z.L. Ren[152], A. Renaud[117], M. Rescigno[133a], S. Resconi[91a], O.L. Rezanova[109,c], P. Reznicek[129],
R. Rezvani[95], R. Richter[101], M. Ridel[80], P. Rieck[16], J. Rieger[54], M. Rijssenbeek[149], A. Rimoldi[121a,121b],
L. Rinaldi[20a], E. Ritsch[62], I. Riu[12], F. Rizatdinova[114], E. Rizvi[76], S.H. Robertson[87,j], A. Robichaud-Veronneau[87],
D. Robinson[28], J.E.M. Robinson[84], A. Robson[53], C. Roda[124a,124b], L. Rodrigues[30], S. Roe[30], O. Røhne[119],
S. Rolli[162], A. Romaniouk[98], M. Romano[20a,20b], E. Romero Adam[168], N. Rompotis[139], M. Ronzani[48], L. Roos[80],
E. Ros[168], S. Rosati[133a], K. Rosbach[49], M. Rose[77], P. Rose[138], P.L. Rosendahl[14], O. Rosenthal[142],
V. Rossetti[147a,147b], E. Rossi[104a,104b], L.P. Rossi[50a], R. Rosten[139], M. Rotaru[26a], I. Roth[173], J. Rothberg[139],
D. Rousseau[117], C.R. Royon[137], A. Rozanov[85], Y. Rozen[153], X. Ruan[146c], F. Rubbo[12], I. Rubinskiy[42], V.I. Rud[99],
C. Rudolph[44], M.S. Rudolph[159], F. Rühr[48], A. Ruiz-Martinez[30], Z. Rurikova[48], N.A. Rusakovich[65], A. Ruschke[100],
J.P. Rutherfoord[7], N. Ruthmann[48], Y.F. Ryabov[123], M. Rybar[129], G. Rybkin[117], N.C. Ryder[120], A.F. Saavedra[151],
G. Sabato[107], S. Sacerdoti[27], A. Saddique[3], I. Sadeh[154], H.F-W. Sadrozinski[138], R. Sadykov[65], F. Safai Tehrani[133a],
H. Sakamoto[156], Y. Sakurai[172], G. Salamanna[135a,135b], A. Salamon[134a], M. Saleem[113], D. Salek[107],
P.H. Sales De Bruin[139], D. Salihagic[101], A. Salnikov[144], J. Salt[168], D. Salvatore[37a,37b], F. Salvatore[150],
A. Salvucci[106], A. Salzburger[30], D. Sampsonidis[155], A. Sanchez[104a,104b], J. Sánchez[168], V. Sanchez Martinez[168],
H. Sandaker[14], R.L. Sandbach[76], H.G. Sander[83], M.P. Sanders[100], M. Sandhoff[176], T. Sandoval[28], C. Sandoval[163],
R. Sandstroem[101], D.P.C. Sankey[131], A. Sansoni[47], C. Santoni[34], R. Santonico[134a,134b], H. Santos[126a],
I. Santoyo Castillo[150], K. Sapp[125], A. Sapronov[65], J.G. Saraiva[126a,126d], B. Sarrazin[21], G. Sartisohn[176], O. Sasaki[66],
Y. Sasaki[156], G. Sauvage[5,∗], E. Sauvan[5], P. Savard[159,e], D.O. Savu[30], C. Sawyer[120], L. Sawyer[79,m], D.H. Saxon[53],
J. Saxon[122], C. Sbarra[20a], A. Sbrizzi[20a,20b], T. Scanlon[78], D.A. Scannicchio[164], M. Scarcella[151], V. Scarfone[37a,37b],
J. Schaarschmidt[173], P. Schacht[101], D. Schaefer[30], R. Schaefer[42], S. Schaepe[21], S. Schaetzel[58b], U. Schäfer[83],
A.C. Schaffer[117], D. Schaile[100], R.D. Schamberger[149], V. Scharf[58a], V.A. Schegelsky[123], D. Scheirich[129],
M. Schernau[164], M.I. Scherzer[35], C. Schiavi[50a,50b], J. Schieck[100], C. Schillo[48], M. Schioppa[37a,37b], S. Schlenker[30],

E. Schmidt[48], K. Schmieden[30], C. Schmitt[83], S. Schmitt[58b], B. Schneider[17], Y.J. Schnellbach[74], U. Schnoor[44],
L. Schoeffel[137], A. Schoening[58b], B.D. Schoenrock[90], A.L.S. Schorlemmer[54], M. Schott[83], D. Schouten[160a],
J. Schovancova[25], S. Schramm[159], M. Schreyer[175], C. Schroeder[83], N. Schuh[83], M.J. Schultens[21],
H.-C. Schultz-Coulon[58a], H. Schulz[16], M. Schumacher[48], B.A. Schumm[138], Ph. Schune[137], C. Schwanenberger[84],
A. Schwartzman[144], T.A. Schwarz[89], Ph. Schwegler[101], Ph. Schwemling[137], R. Schwienhorst[90], J. Schwindling[137],
T. Schwindt[21], M. Schwoerer[5], F.G. Sciacca[17], E. Scifo[117], G. Sciolla[23], W.G. Scott[131], F. Scuri[124a,124b], F. Scutti[21],
J. Searcy[89], G. Sedov[42], E. Sedykh[123], P. Seema[21], S.C. Seidel[105], A. Seiden[138], F. Seifert[128], J.M. Seixas[24a],
G. Sekhniaidze[104a], S.J. Sekula[40], K.E. Selbach[46], D.M. Seliverstov[123,*], G. Sellers[74], N. Semprini-Cesari[20a,20b],
C. Serfon[30], L. Serin[117], L. Serkin[54], T. Serre[85], R. Seuster[160a], H. Severini[113], T. Sfiligoj[75], F. Sforza[101],
A. Sfyrla[30], E. Shabalina[54], M. Shamim[116], L.Y. Shan[33a], R. Shang[166], J.T. Shank[22], M. Shapiro[15], P.B. Shatalov[97],
K. Shaw[165a,165b], C.Y. Shehu[150], P. Sherwood[78], L. Shi[152,ad], S. Shimizu[67], C.O. Shimmin[164], M. Shimojima[102],
M. Shiyakova[65], A. Shmeleva[96], M.J. Shochet[31], D. Short[120], S. Shrestha[64], E. Shulga[98], M.A. Shupe[7],
S. Shushkevich[42], P. Sicho[127], O. Sidiropoulou[155], D. Sidorov[114], A. Sidoti[133a], F. Siegert[44], Dj. Sijacki[13a],
J. Silva[126a,126d], Y. Silver[154], D. Silverstein[144], S.B. Silverstein[147a], V. Simak[128], O. Simard[5], Lj. Simic[13a],
S. Simion[117], E. Simioni[83], B. Simmons[78], D. Simon[34], R. Simoniello[91a,91b], P. Sinervo[159], N.B. Sinev[116],
G. Siragusa[175], A. Sircar[79], A.N. Sisakyan[65,*], S.Yu. Sivoklokov[99], J. Sjölin[147a,147b], T.B. Sjursen[14],
H.P. Skottowe[57], K.Yu. Skovpen[109], P. Skubic[113], M. Slater[18], T. Slavicek[128], M. Slawinska[107], K. Sliwa[162],
V. Smakhtin[173], B.H. Smart[46], L. Smestad[14], S.Yu. Smirnov[98], Y. Smirnov[98], L.N. Smirnova[99,ae], O. Smirnova[81],
K.M. Smith[53], M. Smizanska[72], K. Smolek[128], A.A. Snesarev[96], G. Snidero[76], S. Snyder[25], R. Sobie[170,j],
F. Socher[44], A. Soffer[154], D.A. Soh[152,ad], C.A. Solans[30], M. Solar[128], J. Solc[128], E.Yu. Soldatov[98], U. Soldevila[168],
A.A. Solodkov[130], A. Soloshenko[65], O.V. Solovyanov[130], V. Solovyev[123], P. Sommer[48], H.Y. Song[33b], N. Soni[1],
A. Sood[15], A. Sopczak[128], B. Sopko[128], V. Sopko[128], V. Sorin[12], M. Sosebee[8], R. Soualah[165a,165c], P. Soueid[95],
A.M. Soukharev[109,c], D. South[42], S. Spagnolo[73a,73b], F. Spanò[77], W.R. Spearman[57], F. Spettel[101], R. Spighi[20a],
G. Spigo[30], L.A. Spiller[88], M. Spousta[129], T. Spreitzer[159], B. Spurlock[8], R.D. St. Denis[53,*], S. Staerz[44],
J. Stahlman[122], R. Stamen[58a], S. Stamm[16], E. Stanecka[39], R.W. Stanek[6], C. Stanescu[135a], M. Stanescu-Bellu[42],
M.M. Stanitzki[42], S. Stapnes[119], E.A. Starchenko[130], J. Stark[55], P. Staroba[127], P. Starovoitov[42], R. Staszewski[39],
P. Stavina[145a,*], P. Steinberg[25], B. Stelzer[143], H.J. Stelzer[30], O. Stelzer-Chilton[160a], H. Stenzel[52], S. Stern[101],
G.A. Stewart[53], J.A. Stillings[21], M.C. Stockton[87], M. Stoebe[87], G. Stoicea[26a], P. Stolte[54], S. Stonjek[101],
A.R. Stradling[8], A. Straessner[44], M.E. Stramaglia[17], J. Strandberg[148], S. Strandberg[147a,147b], A. Strandlie[119],
E. Strauss[144], M. Strauss[113], P. Strizenec[145b], R. Ströhmer[175], D.M. Strom[116], R. Stroynowski[40], A. Strubig[106],
S.A. Stucci[17], B. Stugu[14], N.A. Styles[42], D. Su[144], J. Su[125], R. Subramaniam[79], A. Succurro[12], Y. Sugaya[118],
C. Suhr[108], M. Suk[128], V.V. Sulin[96], S. Sultansoy[4d], T. Sumida[68], S. Sun[57], X. Sun[33a], J.E. Sundermann[48],
K. Suruliz[140], G. Susinno[37a,37b], M.R. Sutton[150], Y. Suzuki[66], M. Svatos[127], S. Swedish[169], M. Swiatlowski[144],
I. Sykora[145a], T. Sykora[129], D. Ta[90], C. Taccini[135a,135b], K. Tackmann[42], J. Taenzer[159], A. Taffard[164],
R. Tafirout[160a], N. Taiblum[154], H. Takai[25], R. Takashima[69], H. Takeda[67], T. Takeshita[141], Y. Takubo[66],
M. Talby[85], A.A. Talyshev[109,c], J.Y.C. Tam[175], K.G. Tan[88], J. Tanaka[156], R. Tanaka[117], S. Tanaka[132], S. Tanaka[66],
A.J. Tanasijczuk[143], B.B. Tannenwald[111], N. Tannoury[21], S. Tapprogge[83], S. Tarem[153], F. Tarrade[29],
G.F. Tartarelli[91a], P. Tas[129], M. Tasevsky[127], T. Tashiro[68], E. Tassi[37a,37b], A. Tavares Delgado[126a,126b],
Y. Tayalati[136d], F.E. Taylor[94], G.N. Taylor[88], W. Taylor[160b], F.A. Teischinger[30], M. Teixeira Dias Castanheira[76],
P. Teixeira-Dias[77], K.K. Temming[48], H. Ten Kate[30], P.K. Teng[152], J.J. Teoh[118], S. Terada[66], K. Terashi[156],
J. Terron[82], S. Terzo[101], M. Testa[47], R.J. Teuscher[159,j], J. Therhaag[21], T. Theveneaux-Pelzer[34], J.P. Thomas[18],
J. Thomas-Wilsker[77], E.N. Thompson[35], P.D. Thompson[18], P.D. Thompson[159], R.J. Thompson[84],
A.S. Thompson[53], L.A. Thomsen[36], E. Thomson[122], M. Thomson[28], W.M. Thong[88], R.P. Thun[89,*], F. Tian[35],
M.J. Tibbetts[15], V.O. Tikhomirov[96,af], Yu.A. Tikhonov[109,c], S. Timoshenko[98], E. Tiouchichine[85], P. Tipton[177],
S. Tisserant[85], T. Todorov[5], S. Todorova-Nova[129], J. Tojo[70], S. Tokár[145a], K. Tokushuku[66], K. Tollefson[90],
E. Tolley[57], L. Tomlinson[84], M. Tomoto[103], L. Tompkins[31], K. Toms[105], N.D. Topilin[65], E. Torrence[116],
H. Torres[143], E. Torró Pastor[168], J. Toth[85,ag], F. Touchard[85], D.R. Tovey[140], H.L. Tran[117], T. Trefzger[175],
L. Tremblet[30], A. Tricoli[30], I.M. Trigger[160a], S. Trincaz-Duvoid[80], M.F. Tripiana[12], W. Trischuk[159], B. Trocmé[55],
C. Troncon[91a], M. Trottier-McDonald[15], M. Trovatelli[135a,135b], P. True[90], M. Trzebinski[39], A. Trzupek[39],
C. Tsarouchas[30], J.C-L. Tseng[120], P.V. Tsiareshka[92], D. Tsionou[137], G. Tsipolitis[10], N. Tsirintanis[9],
S. Tsiskaridze[12], V. Tsiskaridze[48], E.G. Tskhadadze[51a], I.I. Tsukerman[97], V. Tsulaia[15], S. Tsuno[66],
D. Tsybychev[149], A. Tudorache[26a], V. Tudorache[26a], A.N. Tuna[122], S.A. Tupputi[20a,20b], S. Turchikhin[99,ae],
D. Turecek[128], I. Turk Cakir[4c], R. Turra[91a,91b], A.J. Turvey[40], P.M. Tuts[35], A. Tykhonov[49], M. Tylmad[147a,147b],
M. Tyndel[131], K. Uchida[21], I. Ueda[156], R. Ueno[29], M. Ughetto[85], M. Ugland[14], M. Uhlenbrock[21], F. Ukegawa[161],
G. Unal[30], A. Undrus[25], G. Unel[164], F.C. Ungaro[48], Y. Unno[66], C. Unverdorben[100], D. Urbaniec[35], P. Urquijo[88],
G. Usai[8], A. Usanova[62], L. Vacavant[85], V. Vacek[128], B. Vachon[87], N. Valencic[107], S. Valentinetti[20a,20b],
A. Valero[168], L. Valery[34], S. Valkar[129], E. Valladolid Gallego[168], S. Vallecorsa[49], J.A. Valls Ferrer[168],
W. Van Den Wollenberg[107], P.C. Van Der Deijl[107], R. van der Geer[107], H. van der Graaf[107], R. Van Der Leeuw[107],

D. van der Ster[30], N. van Eldik[30], P. van Gemmeren[6], J. Van Nieuwkoop[143], I. van Vulpen[107], M.C. van Woerden[30], M. Vanadia[133a,133b], W. Vandelli[30], R. Vanguri[122], A. Vaniachine[6], P. Vankov[42], F. Vannucci[80], G. Vardanyan[178], R. Vari[133a], E.W. Varnes[7], T. Varol[86], D. Varouchas[80], A. Vartapetian[8], K.E. Varvell[151], F. Vazeille[34], T. Vazquez Schroeder[54], J. Veatch[7], F. Veloso[126a,126c], S. Veneziano[133a], A. Ventura[73a,73b], D. Ventura[86], M. Venturi[170], N. Venturi[159], A. Venturini[23], V. Vercesi[121a], M. Verducci[133a,133b], W. Verkerke[107], J.C. Vermeulen[107], A. Vest[44], M.C. Vetterli[143,e], O. Viazlo[81], I. Vichou[166], T. Vickey[146c,ah], O.E. Vickey Boeriu[146c], G.H.A. Viehhauser[120], S. Viel[169], R. Vigne[30], M. Villa[20a,20b], M. Villaplana Perez[91a,91b], E. Vilucchi[47], M.G. Vincter[29], V.B. Vinogradov[65], J. Virzi[15], I. Vivarelli[150], F. Vives Vaque[3], S. Vlachos[10], D. Vladoiu[100], M. Vlasak[128], A. Vogel[21], M. Vogel[32a], P. Vokac[128], G. Volpi[124a,124b], M. Volpi[88], H. von der Schmitt[101], H. von Radziewski[48], E. von Toerne[21], V. Vorobel[129], K. Vorobev[98], M. Vos[168], R. Voss[30], J.H. Vossebeld[74], N. Vranjes[137], M. Vranjes Milosavljevic[13a], V. Vrba[127], M. Vreeswijk[107], T. Vu Anh[48], R. Vuillermet[30], I. Vukotic[31], Z. Vykydal[128], P. Wagner[21], W. Wagner[176], H. Wahlberg[71], S. Wahrmund[44], J. Wakabayashi[103], J. Walder[72], R. Walker[100], W. Walkowiak[142], R. Wall[177], P. Waller[74], B. Walsh[177], C. Wang[152,ai], C. Wang[45], F. Wang[174], H. Wang[15], H. Wang[40], J. Wang[42], J. Wang[33a], K. Wang[87], R. Wang[105], S.M. Wang[152], T. Wang[21], X. Wang[177], C. Wanotayaroj[116], A. Warburton[87], C.P. Ward[28], D.R. Wardrope[78], M. Warsinsky[48], A. Washbrook[46], C. Wasicki[42], P.M. Watkins[18], A.T. Watson[18], I.J. Watson[151], M.F. Watson[18], G. Watts[139], S. Watts[84], B.M. Waugh[78], S. Webb[84], M.S. Weber[17], S.W. Weber[175], J.S. Webster[31], A.R. Weidberg[120], B. Weinert[61], J. Weingarten[54], C. Weiser[48], H. Weits[107], P.S. Wells[30], T. Wenaus[25], D. Wendland[16], Z. Weng[152,ad], T. Wengler[30], S. Wenig[30], N. Wermes[21], M. Werner[48], P. Werner[30], M. Wessels[58a], J. Wetter[162], K. Whalen[29], A. White[8], M.J. White[1], R. White[32b], S. White[124a,124b], D. Whiteson[164], D. Wicke[176], F.J. Wickens[131], W. Wiedenmann[174], M. Wielers[131], P. Wienemann[21], C. Wiglesworth[36], L.A.M. Wiik-Fuchs[21], P.A. Wijeratne[78], A. Wildauer[101], M.A. Wildt[42,aj], H.G. Wilkens[30], H.H. Williams[122], S. Williams[28], C. Willis[90], S. Willocq[86], A. Wilson[89], J.A. Wilson[18], I. Wingerter-Seez[5], F. Winklmeier[116], B.T. Winter[21], M. Wittgen[144], T. Wittig[43], J. Wittkowski[100], S.J. Wollstadt[83], M.W. Wolter[39], H. Wolters[126a,126c], B.K. Wosiek[39], J. Wotschack[30], M.J. Woudstra[84], K.W. Wozniak[39], M. Wright[53], M. Wu[55], S.L. Wu[174], X. Wu[49], Y. Wu[89], E. Wulf[35], T.R. Wyatt[84], B.M. Wynne[46], S. Xella[36], M. Xiao[137], D. Xu[33a], L. Xu[33b,ak], B. Yabsley[151], S. Yacoob[146b,al], R. Yakabe[67], M. Yamada[66], H. Yamaguchi[156], Y. Yamaguchi[118], A. Yamamoto[66], S. Yamamoto[156], T. Yamamura[156], T. Yamanaka[156], K. Yamauchi[103], Y. Yamazaki[67], Z. Yan[22], H. Yang[33e], H. Yang[174], U.K. Yang[84], Y. Yang[111], S. Yanush[93], L. Yao[33a], W-M. Yao[15], Y. Yasu[66], E. Yatsenko[42], K.H. Yau Wong[21], J. Ye[40], S. Ye[25], I. Yeletskikh[65], A.L. Yen[57], E. Yildirim[42], M. Yilmaz[4b], R. Yoosoofmiya[125], K. Yorita[172], R. Yoshida[6], K. Yoshihara[156], C. Young[144], C.J.S. Young[30], S. Youssef[22], D.R. Yu[15], J. Yu[8], J.M. Yu[89], J. Yu[114], L. Yuan[67], A. Yurkewicz[108], I. Yusuff[28,am], B. Zabinski[39], R. Zaidan[63], A.M. Zaitsev[130,z], A. Zaman[149], S. Zambito[23], L. Zanello[133a,133b], D. Zanzi[88], C. Zeitnitz[176], M. Zeman[128], A. Zemla[38a], K. Zengel[23], O. Zenin[130], T. Ženiš[145a], D. Zerwas[117], G. Zevi della Porta[57], D. Zhang[89], F. Zhang[174], H. Zhang[90], J. Zhang[6], L. Zhang[152], R. Zhang[33b], X. Zhang[33d], Z. Zhang[117], Y. Zhao[33d], Z. Zhao[33b], A. Zhemchugov[65], J. Zhong[120], B. Zhou[89], L. Zhou[35], N. Zhou[164], C.G. Zhu[33d], H. Zhu[33a], J. Zhu[89], Y. Zhu[33b], X. Zhuang[33a], K. Zhukov[96], A. Zibell[175], D. Zieminska[61], N.I. Zimine[65], C. Zimmermann[83], R. Zimmermann[21], S. Zimmermann[21], S. Zimmermann[48], Z. Zinonos[54], M. Ziolkowski[142], G. Zobernig[174], A. Zoccoli[20a,20b], M. zur Nedden[16], G. Zurzolo[104a,104b], V. Zutshi[108], L. Zwalinski[30].

[1] Department of Physics, University of Adelaide, Adelaide, Australia

[2] Physics Department, SUNY Albany, Albany NY, United States of America

[3] Department of Physics, University of Alberta, Edmonton AB, Canada

[4] [(a)] Department of Physics, Ankara University, Ankara; [(b)] Department of Physics, Gazi University, Ankara; [(c)] Istanbul Aydin University, Istanbul; [(d)] Division of Physics, TOBB University of Economics and Technology, Ankara, Turkey

[5] LAPP, CNRS/IN2P3 and Université de Savoie, Annecy-le-Vieux, France

[6] High Energy Physics Division, Argonne National Laboratory, Argonne IL, United States of America

[7] Department of Physics, University of Arizona, Tucson AZ, United States of America

[8] Department of Physics, The University of Texas at Arlington, Arlington TX, United States of America

[9] Physics Department, University of Athens, Athens, Greece

[10] Physics Department, National Technical University of Athens, Zografou, Greece

[11] Institute of Physics, Azerbaijan Academy of Sciences, Baku, Azerbaijan

[12] Institut de Física d'Altes Energies and Departament de Física de la Universitat Autònoma de Barcelona, Barcelona, Spain

[13] [(a)] Institute of Physics, University of Belgrade, Belgrade; [(b)] Vinca Institute of Nuclear Sciences, University of Belgrade, Belgrade, Serbia

[14] Department for Physics and Technology, University of Bergen, Bergen, Norway

[15] Physics Division, Lawrence Berkeley National Laboratory and University of California, Berkeley CA, United

States of America

[16] Department of Physics, Humboldt University, Berlin, Germany

[17] Albert Einstein Center for Fundamental Physics and Laboratory for High Energy Physics, University of Bern, Bern, Switzerland

[18] School of Physics and Astronomy, University of Birmingham, Birmingham, United Kingdom

[19] [a] Department of Physics, Bogazici University, Istanbul; [b] Department of Physics, Dogus University, Istanbul; [c] Department of Physics Engineering, Gaziantep University, Gaziantep, Turkey

[20] [a] INFN Sezione di Bologna; [b] Dipartimento di Fisica e Astronomia, Università di Bologna, Bologna, Italy

[21] Physikalisches Institut, University of Bonn, Bonn, Germany

[22] Department of Physics, Boston University, Boston MA, United States of America

[23] Department of Physics, Brandeis University, Waltham MA, United States of America

[24] [a] Universidade Federal do Rio De Janeiro COPPE/EE/IF, Rio de Janeiro; [b] Federal University of Juiz de Fora (UFJF), Juiz de Fora; [c] Federal University of Sao Joao del Rei (UFSJ), Sao Joao del Rei; [d] Instituto de Fisica, Universidade de Sao Paulo, Sao Paulo, Brazil

[25] Physics Department, Brookhaven National Laboratory, Upton NY, United States of America

[26] [a] National Institute of Physics and Nuclear Engineering, Bucharest; [b] National Institute for Research and Development of Isotopic and Molecular Technologies, Physics Department, Cluj Napoca; [c] University Politehnica Bucharest, Bucharest; [d] West University in Timisoara, Timisoara, Romania

[27] Departamento de Física, Universidad de Buenos Aires, Buenos Aires, Argentina

[28] Cavendish Laboratory, University of Cambridge, Cambridge, United Kingdom

[29] Department of Physics, Carleton University, Ottawa ON, Canada

[30] CERN, Geneva, Switzerland

[31] Enrico Fermi Institute, University of Chicago, Chicago IL, United States of America

[32] [a] Departamento de Física, Pontificia Universidad Católica de Chile, Santiago; [b] Departamento de Física, Universidad Técnica Federico Santa María, Valparaíso, Chile

[33] [a] Institute of High Energy Physics, Chinese Academy of Sciences, Beijing; [b] Department of Modern Physics, University of Science and Technology of China, Anhui; [c] Department of Physics, Nanjing University, Jiangsu; [d] School of Physics, Shandong University, Shandong; [e] Physics Department, Shanghai Jiao Tong University, Shanghai; [f] Physics Department, Tsinghua University, Beijing 100084, China

[34] Laboratoire de Physique Corpusculaire, Clermont Université and Université Blaise Pascal and CNRS/IN2P3, Clermont-Ferrand, France

[35] Nevis Laboratory, Columbia University, Irvington NY, United States of America

[36] Niels Bohr Institute, University of Copenhagen, Kobenhavn, Denmark

[37] [a] INFN Gruppo Collegato di Cosenza, Laboratori Nazionali di Frascati; [b] Dipartimento di Fisica, Università della Calabria, Rende, Italy

[38] [a] AGH University of Science and Technology, Faculty of Physics and Applied Computer Science, Krakow; [b] Marian Smoluchowski Institute of Physics, Jagiellonian University, Krakow, Poland

[39] The Henryk Niewodniczanski Institute of Nuclear Physics, Polish Academy of Sciences, Krakow, Poland

[40] Physics Department, Southern Methodist University, Dallas TX, United States of America

[41] Physics Department, University of Texas at Dallas, Richardson TX, United States of America

[42] DESY, Hamburg and Zeuthen, Germany

[43] Institut für Experimentelle Physik IV, Technische Universität Dortmund, Dortmund, Germany

[44] Institut für Kern- und Teilchenphysik, Technische Universität Dresden, Dresden, Germany

[45] Department of Physics, Duke University, Durham NC, United States of America

[46] SUPA - School of Physics and Astronomy, University of Edinburgh, Edinburgh, United Kingdom

[47] INFN Laboratori Nazionali di Frascati, Frascati, Italy

[48] Fakultät für Mathematik und Physik, Albert-Ludwigs-Universität, Freiburg, Germany

[49] Section de Physique, Université de Genève, Geneva, Switzerland

[50] [a] INFN Sezione di Genova; [b] Dipartimento di Fisica, Università di Genova, Genova, Italy

[51] [a] E. Andronikashvili Institute of Physics, Iv. Javakhishvili Tbilisi State University, Tbilisi; [b] High Energy Physics Institute, Tbilisi State University, Tbilisi, Georgia

[52] II Physikalisches Institut, Justus-Liebig-Universität Giessen, Giessen, Germany

[53] SUPA - School of Physics and Astronomy, University of Glasgow, Glasgow, United Kingdom

[54] II Physikalisches Institut, Georg-August-Universität, Göttingen, Germany

[55] Laboratoire de Physique Subatomique et de Cosmologie, Université Grenoble-Alpes, CNRS/IN2P3, Grenoble, France

[56] Department of Physics, Hampton University, Hampton VA, United States of America

[57] Laboratory for Particle Physics and Cosmology, Harvard University, Cambridge MA, United States of America

[58] [a] Kirchhoff-Institut für Physik, Ruprecht-Karls-Universität Heidelberg, Heidelberg; [b] Physikalisches Institut, Ruprecht-Karls-Universität Heidelberg, Heidelberg; [c] ZITI Institut für technische Informatik, Ruprecht-Karls-Universität Heidelberg, Mannheim, Germany

[59] Faculty of Applied Information Science, Hiroshima Institute of Technology, Hiroshima, Japan

[60] [a] Department of Physics, The Chinese University of Hong Kong, Shatin, N.T., Hong Kong; [b] Department of Physics, The University of Hong Kong, Hong Kong; [c] Department of Physics, The Hong Kong University of Science and Technology, Clear Water Bay, Kowloon, Hong Kong, China

[61] Department of Physics, Indiana University, Bloomington IN, United States of America

[62] Institut für Astro- und Teilchenphysik, Leopold-Franzens-Universität, Innsbruck, Austria

[63] University of Iowa, Iowa City IA, United States of America

[64] Department of Physics and Astronomy, Iowa State University, Ames IA, United States of America

[65] Joint Institute for Nuclear Research, JINR Dubna, Dubna, Russia

[66] KEK, High Energy Accelerator Research Organization, Tsukuba, Japan

[67] Graduate School of Science, Kobe University, Kobe, Japan

[68] Faculty of Science, Kyoto University, Kyoto, Japan

[69] Kyoto University of Education, Kyoto, Japan

[70] Department of Physics, Kyushu University, Fukuoka, Japan

[71] Instituto de Física La Plata, Universidad Nacional de La Plata and CONICET, La Plata, Argentina

[72] Physics Department, Lancaster University, Lancaster, United Kingdom

[73] [a] INFN Sezione di Lecce; [b] Dipartimento di Matematica e Fisica, Università del Salento, Lecce, Italy

[74] Oliver Lodge Laboratory, University of Liverpool, Liverpool, United Kingdom

[75] Department of Physics, Jožef Stefan Institute and University of Ljubljana, Ljubljana, Slovenia

[76] School of Physics and Astronomy, Queen Mary University of London, London, United Kingdom

[77] Department of Physics, Royal Holloway University of London, Surrey, United Kingdom

[78] Department of Physics and Astronomy, University College London, London, United Kingdom

[79] Louisiana Tech University, Ruston LA, United States of America

[80] Laboratoire de Physique Nucléaire et de Hautes Energies, UPMC and Université Paris-Diderot and CNRS/IN2P3, Paris, France

[81] Fysiska institutionen, Lunds universitet, Lund, Sweden

[82] Departamento de Fisica Teorica C-15, Universidad Autonoma de Madrid, Madrid, Spain

[83] Institut für Physik, Universität Mainz, Mainz, Germany

[84] School of Physics and Astronomy, University of Manchester, Manchester, United Kingdom

[85] CPPM, Aix-Marseille Université and CNRS/IN2P3, Marseille, France

[86] Department of Physics, University of Massachusetts, Amherst MA, United States of America

[87] Department of Physics, McGill University, Montreal QC, Canada

[88] School of Physics, University of Melbourne, Victoria, Australia

[89] Department of Physics, The University of Michigan, Ann Arbor MI, United States of America

[90] Department of Physics and Astronomy, Michigan State University, East Lansing MI, United States of America

[91] [a] INFN Sezione di Milano; [b] Dipartimento di Fisica, Università di Milano, Milano, Italy

[92] B.I. Stepanov Institute of Physics, National Academy of Sciences of Belarus, Minsk, Republic of Belarus

[93] National Scientific and Educational Centre for Particle and High Energy Physics, Minsk, Republic of Belarus

[94] Department of Physics, Massachusetts Institute of Technology, Cambridge MA, United States of America

[95] Group of Particle Physics, University of Montreal, Montreal QC, Canada

[96] P.N. Lebedev Institute of Physics, Academy of Sciences, Moscow, Russia

[97] Institute for Theoretical and Experimental Physics (ITEP), Moscow, Russia

[98] National Research Nuclear University MEPhI, Moscow, Russia

[99] D.V.Skobeltsyn Institute of Nuclear Physics, M.V.Lomonosov Moscow State University, Moscow, Russia

[100] Fakultät für Physik, Ludwig-Maximilians-Universität München, München, Germany

[101] Max-Planck-Institut für Physik (Werner-Heisenberg-Institut), München, Germany

[102] Nagasaki Institute of Applied Science, Nagasaki, Japan

[103] Graduate School of Science and Kobayashi-Maskawa Institute, Nagoya University, Nagoya, Japan

[104] [a] INFN Sezione di Napoli; [b] Dipartimento di Fisica, Università di Napoli, Napoli, Italy

[105] Department of Physics and Astronomy, University of New Mexico, Albuquerque NM, United States of America

[106] Institute for Mathematics, Astrophysics and Particle Physics, Radboud University Nijmegen/Nikhef, Nijmegen, Netherlands

[107] Nikhef National Institute for Subatomic Physics and University of Amsterdam, Amsterdam, Netherlands

[108] Department of Physics, Northern Illinois University, DeKalb IL, United States of America

[109] Budker Institute of Nuclear Physics, SB RAS, Novosibirsk, Russia

[110] Department of Physics, New York University, New York NY, United States of America

[111] Ohio State University, Columbus OH, United States of America

[112] Faculty of Science, Okayama University, Okayama, Japan

[113] Homer L. Dodge Department of Physics and Astronomy, University of Oklahoma, Norman OK, United States of America

[114] Department of Physics, Oklahoma State University, Stillwater OK, United States of America

[115] Palacký University, RCPTM, Olomouc, Czech Republic

[116] Center for High Energy Physics, University of Oregon, Eugene OR, United States of America

[117] LAL, Université Paris-Sud and CNRS/IN2P3, Orsay, France

[118] Graduate School of Science, Osaka University, Osaka, Japan

[119] Department of Physics, University of Oslo, Oslo, Norway

[120] Department of Physics, Oxford University, Oxford, United Kingdom

[121] [a] INFN Sezione di Pavia; [b] Dipartimento di Fisica, Università di Pavia, Pavia, Italy

[122] Department of Physics, University of Pennsylvania, Philadelphia PA, United States of America

[123] Petersburg Nuclear Physics Institute, Gatchina, Russia

[124] [a] INFN Sezione di Pisa; [b] Dipartimento di Fisica E. Fermi, Università di Pisa, Pisa, Italy

[125] Department of Physics and Astronomy, University of Pittsburgh, Pittsburgh PA, United States of America

[126] [a] Laboratorio de Instrumentacao e Fisica Experimental de Particulas - LIP, Lisboa; [b] Faculdade de Ciências, Universidade de Lisboa, Lisboa; [c] Department of Physics, University of Coimbra, Coimbra; [d] Centro de Física Nuclear da Universidade de Lisboa, Lisboa; [e] Departamento de Fisica, Universidade do Minho, Braga; [f] Departamento de Fisica Teorica y del Cosmos and CAFPE, Universidad de Granada, Granada (Spain); [g] Dep Fisica and CEFITEC of Faculdade de Ciencias e Tecnologia, Universidade Nova de Lisboa, Caparica, Portugal

[127] Institute of Physics, Academy of Sciences of the Czech Republic, Praha, Czech Republic

[128] Czech Technical University in Prague, Praha, Czech Republic

[129] Faculty of Mathematics and Physics, Charles University in Prague, Praha, Czech Republic

[130] State Research Center Institute for High Energy Physics, Protvino, Russia

[131] Particle Physics Department, Rutherford Appleton Laboratory, Didcot, United Kingdom

[132] Ritsumeikan University, Kusatsu, Shiga, Japan

[133] [a] INFN Sezione di Roma; [b] Dipartimento di Fisica, Sapienza Università di Roma, Roma, Italy

[134] [a] INFN Sezione di Roma Tor Vergata; [b] Dipartimento di Fisica, Università di Roma Tor Vergata, Roma, Italy

[135] [a] INFN Sezione di Roma Tre; [b] Dipartimento di Matematica e Fisica, Università Roma Tre, Roma, Italy

[136] [a] Faculté des Sciences Ain Chock, Réseau Universitaire de Physique des Hautes Energies - Université Hassan II, Casablanca; [b] Centre National de l'Energie des Sciences Techniques Nucleaires, Rabat; [c] Faculté des Sciences Semlalia, Université Cadi Ayyad, LPHEA-Marrakech; [d] Faculté des Sciences, Université Mohamed Premier and LPTPM, Oujda; [e] Faculté des sciences, Université Mohammed V-Agdal, Rabat, Morocco

[137] DSM/IRFU (Institut de Recherches sur les Lois Fondamentales de l'Univers), CEA Saclay (Commissariat à l'Energie Atomique et aux Energies Alternatives), Gif-sur-Yvette, France

[138] Santa Cruz Institute for Particle Physics, University of California Santa Cruz, Santa Cruz CA, United States of America

[139] Department of Physics, University of Washington, Seattle WA, United States of America

[140] Department of Physics and Astronomy, University of Sheffield, Sheffield, United Kingdom

[141] Department of Physics, Shinshu University, Nagano, Japan

[142] Fachbereich Physik, Universität Siegen, Siegen, Germany

[143] Department of Physics, Simon Fraser University, Burnaby BC, Canada

[144] SLAC National Accelerator Laboratory, Stanford CA, United States of America

[145] [a] Faculty of Mathematics, Physics & Informatics, Comenius University, Bratislava; [b] Department of Subnuclear Physics, Institute of Experimental Physics of the Slovak Academy of Sciences, Kosice, Slovak Republic

[146] [a] Department of Physics, University of Cape Town, Cape Town; [b] Department of Physics, University of Johannesburg, Johannesburg; [c] School of Physics, University of the Witwatersrand, Johannesburg, South Africa

[147] [a] Department of Physics, Stockholm University; [b] The Oskar Klein Centre, Stockholm, Sweden

[148] Physics Department, Royal Institute of Technology, Stockholm, Sweden

[149] Departments of Physics & Astronomy and Chemistry, Stony Brook University, Stony Brook NY, United States of America

[150] Department of Physics and Astronomy, University of Sussex, Brighton, United Kingdom

[151] School of Physics, University of Sydney, Sydney, Australia

[152] Institute of Physics, Academia Sinica, Taipei, Taiwan

[153] Department of Physics, Technion: Israel Institute of Technology, Haifa, Israel

[154] Raymond and Beverly Sackler School of Physics and Astronomy, Tel Aviv University, Tel Aviv, Israel

[155] Department of Physics, Aristotle University of Thessaloniki, Thessaloniki, Greece

[156] International Center for Elementary Particle Physics and Department of Physics, The University of Tokyo, Tokyo, Japan

[157] Graduate School of Science and Technology, Tokyo Metropolitan University, Tokyo, Japan

[158] Department of Physics, Tokyo Institute of Technology, Tokyo, Japan

[159] Department of Physics, University of Toronto, Toronto ON, Canada

[160] [a] TRIUMF, Vancouver BC; [b] Department of Physics and Astronomy, York University, Toronto ON, Canada

[161] Faculty of Pure and Applied Sciences, University of Tsukuba, Tsukuba, Japan

[162] Department of Physics and Astronomy, Tufts University, Medford MA, United States of America

[163] Centro de Investigaciones, Universidad Antonio Narino, Bogota, Colombia

[164] Department of Physics and Astronomy, University of California Irvine, Irvine CA, United States of America

[165] [a] INFN Gruppo Collegato di Udine, Sezione di Trieste, Udine; [b] ICTP, Trieste; [c] Dipartimento di Chimica, Fisica e Ambiente, Università di Udine, Udine, Italy

[166] Department of Physics, University of Illinois, Urbana IL, United States of America

[167] Department of Physics and Astronomy, University of Uppsala, Uppsala, Sweden

[168] Instituto de Física Corpuscular (IFIC) and Departamento de Física Atómica, Molecular y Nuclear and Departamento de Ingeniería Electrónica and Instituto de Microelectrónica de Barcelona (IMB-CNM), University of Valencia and CSIC, Valencia, Spain

[169] Department of Physics, University of British Columbia, Vancouver BC, Canada

[170] Department of Physics and Astronomy, University of Victoria, Victoria BC, Canada

[171] Department of Physics, University of Warwick, Coventry, United Kingdom

[172] Waseda University, Tokyo, Japan

[173] Department of Particle Physics, The Weizmann Institute of Science, Rehovot, Israel

[174] Department of Physics, University of Wisconsin, Madison WI, United States of America

[175] Fakultät für Physik und Astronomie, Julius-Maximilians-Universität, Würzburg, Germany

[176] Fachbereich C Physik, Bergische Universität Wuppertal, Wuppertal, Germany

[177] Department of Physics, Yale University, New Haven CT, United States of America

[178] Yerevan Physics Institute, Yerevan, Armenia

[179] Centre de Calcul de l'Institut National de Physique Nucléaire et de Physique des Particules (IN2P3), Villeurbanne, France

[a] Also at Department of Physics, King's College London, London, United Kingdom

[b] Also at Institute of Physics, Azerbaijan Academy of Sciences, Baku, Azerbaijan

[c] Also at Novosibirsk State University, Novosibirsk, Russia

[d] Also at Particle Physics Department, Rutherford Appleton Laboratory, Didcot, United Kingdom

[e] Also at TRIUMF, Vancouver BC, Canada

[f] Also at Department of Physics, California State University, Fresno CA, United States of America

[g] Also at Tomsk State University, Tomsk, Russia

[h] Also at CPPM, Aix-Marseille Université and CNRS/IN2P3, Marseille, France

[i] Also at Università di Napoli Parthenope, Napoli, Italy

[j] Also at Institute of Particle Physics (IPP), Canada

[k] Also at Department of Physics, St. Petersburg State Polytechnical University, St. Petersburg, Russia

[l] Also at Department of Financial and Management Engineering, University of the Aegean, Chios, Greece

[m] Also at Louisiana Tech University, Ruston LA, United States of America

[n] Also at Institucio Catalana de Recerca i Estudis Avancats, ICREA, Barcelona, Spain

[o] Also at Department of Physics, The University of Texas at Austin, Austin TX, United States of America

[p] Also at Institute of Theoretical Physics, Ilia State University, Tbilisi, Georgia

[q] Also at CERN, Geneva, Switzerland

[r] Also at Ochadai Academic Production, Ochanomizu University, Tokyo, Japan

[s] Also at Manhattan College, New York NY, United States of America

[t] Also at Institute of Physics, Academia Sinica, Taipei, Taiwan

[u] Also at LAL, Université Paris-Sud and CNRS/IN2P3, Orsay, France

[v] Also at Academia Sinica Grid Computing, Institute of Physics, Academia Sinica, Taipei, Taiwan

[w] Also at Laboratoire de Physique Nucléaire et de Hautes Energies, UPMC and Université Paris-Diderot and CNRS/IN2P3, Paris, France

[x] Also at School of Physical Sciences, National Institute of Science Education and Research, Bhubaneswar, India

[y] Also at Dipartimento di Fisica, Sapienza Università di Roma, Roma, Italy

[z] Also at Moscow Institute of Physics and Technology State University, Dolgoprudny, Russia

[aa] Also at Section de Physique, Université de Genève, Geneva, Switzerland

[ab] Also at International School for Advanced Studies (SISSA), Trieste, Italy

[ac] Also at Department of Physics and Astronomy, University of South Carolina, Columbia SC, United States of America

[ad] Also at School of Physics and Engineering, Sun Yat-sen University, Guangzhou, China

[ae] Also at Faculty of Physics, M.V.Lomonosov Moscow State University, Moscow, Russia

[af] Also at National Research Nuclear University MEPhI, Moscow, Russia

[ag] Also at Institute for Particle and Nuclear Physics, Wigner Research Centre for Physics, Budapest, Hungary

[ah] Also at Department of Physics, Oxford University, Oxford, United Kingdom

[ai] Also at Department of Physics, Nanjing University, Jiangsu, China

[aj] Also at Institut für Experimentalphysik, Universität Hamburg, Hamburg, Germany

[ak] Also at Department of Physics, The University of Michigan, Ann Arbor MI, United States of America

[al] Also at Discipline of Physics, University of KwaZulu-Natal, Durban, South Africa

[am] Also at University of Malaya, Department of Physics, Kuala Lumpur, Malaysia

* Deceased